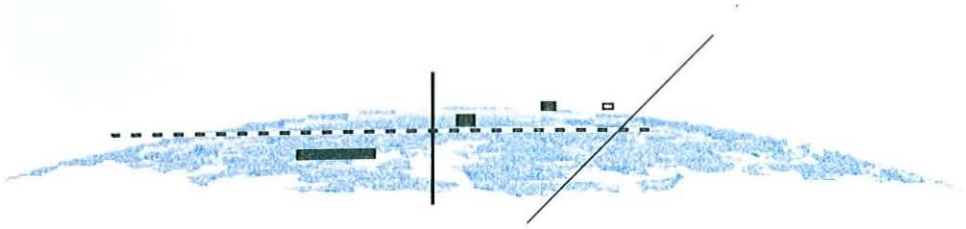

GeoForschungsZentrum Potsdam
STIFTUNG DES ÖFFENTLICHEN RECHTS

Ludwig Ballani
Hans Greiner-Mai
Dietrich Stromeyer

Determining the Magnetic Field in the Earth's Deep Mantle by an Inverse Boundary Value Problem

Scientific Technical Report STR99/12

Imprint

GeoForschungsZentrum Potsdam
Telegrafenberg
D-14473 Potsdam

e-mail: postmaster@gfz-potsdam.de
www: http://www.gfz-potsdam.de

Printed in Potsdam/Germany
August 1999

Ludwig Ballani,
Hans Greiner-Mai, Dietrich Stromeyer

Determining the Magnetic Field in the Earth's Deep Mantle by an Inverse Boundary Value Problem

Scientific Technical Report STR99/12

SUMMARY

The earth rotation and the geomagnetic field are clearly correlated in the decade period interval (10 y...100 y). A considerable part of this correlation can be explained by core-mantle coupling. The magnetic field influences the mantle rotation if the electric conductivity of the mantle is sufficiently high (electromagnetic coupling) or indicates variations in the velocity field of the outermost core which are related to topographic torques on the mantle if the shape of the core-mantle boundary is irregular (topographic coupling). A part of the observed time lag between the variations of the geomagnetic field and the length of day is associated with the inertia of the coupled bodies. The other part is caused by the diffusion of the time-variable geomagnetic field through the electrically conducting mantle. The investigation of the core-mantle coupling torques and the interpretation of the observed time lag require the calculation of the temporally variable magnetic field within the mantle and at the core-mantle boundary by solving the magnetic induction equation.

The earth mantle is assumed to be a two-layer spherical shell, whose inner layer is electrically conducting. We only consider the poloidal part of the magnetic field with boundary values which are conventionally given by a spherical harmonic expansion of the observed geomagnetic potential field on the earth surface. Thus, we are concerned with a one-side-data supported problem (non-characteristic Cauchy problem), which is well known as an extremely ill-posed inverse boundary value problem in heat conduction theory. Its solution requires a stabilizing technique which should be theoretically based.

We develop a regularizing solution procedure accounting for recent theoretical stability estimates. The capabilities of the procedure are shown for a single magnetic field component of the spherical harmonic field expansion beginning from the year 1900 by varying the mantle conductivity model and the degree of smoothness in the regularization. As an example, the radial component of a global (5,5) core-mantle boundary field is calculated for two epochs.

Scientific Technical Report STR 99/12
DOI: 10.2312/GFZ.b103-99127

1. INTRODUCTION

Various geophysical problems are strongly connected with the behaviour of the geomagnetic field within the mantle and on the core-mantle boundary (CMB). A particular problem, for which the magnetic field behaviour is studied in this paper, is the *origin of the decade variations of the length of day* (ΔLOD). Other related problems are the determination of the *boundary values for dynamo models*, estimates of the *velocity field in the outer core* according to the frozen-field theory, and the *penetration of harmonic modes* of the magnetic field through the mantle (geomagnetic induction).

Several authors (e.g., Munk & Revelle 1952, Lambeck & Cazenave 1976, Jochmann & Greiner-Mai 1996) have shown that atmospheric processes can excite only a small part of decade ΔLOD and have suggested that the larger part must be attributed to *processes within the earth core*, which *influence the earth rotation* by exciting core-mantle coupling torques on the mantle. This suggestion is based on the strong correlations between ΔLOD and the geomagnetic field variations for periods of about 20, 30 and 70 years.

The hypothesis that the *electromagnetic core-mantle coupling* is responsible for the length of day variation has been suggested implicitely first by Bullard *et al.* (1950) and more thoroughly first by Rochester (1960). He proves that Lorentz torques of sufficiently high magnitude (about 10^{17} Nm) on the mantle can be produced if the mean conductivity in a spherical shell of 2000 km thickness enclosing the core is in the order of 100 Sm^{-1}.

A different type of coupling is the *topographic coupling* based on the interaction between the velocity field of the outer core and the irregularities of the CMB. Estimates of the associated pressure torques (about 10^{18} Nm) indicate that they may be responsible for the variation of polar motion but are too large for ΔLOD (e.g. Hinderer *et al.* 1990; Jault & Le Mouël 1990). The electromagnetic coupling torques are conventionally calculated from the (non-potential) geomagnetic field within the mantle. The pressure torques are derived from the velocity field of the outer core, which can be estimated using the frozen-field approximation of the induction equation of the outer core (e.g. Backus 1968; Braginsky 1984; Gire & Le Mouël 1990; Whaler & Davis 1997). A review of coupling mechanisms is given by Le Mouël, Hulot & Poirier (1997). The toroidal part of the geomagnetic field within the mantle determines an important part of the electromagnetic torques, but it cannot be observed on the earth surface. However, boundary values of the toroidal field according to field advection can be inferred from the velocity field at the CMB (e.g. Stix & Roberts 1984). Thus, the *poloidal geomagnetic field at the CMB* enters both types of torques considered and must be known there

Scientific Technical Report STR 99/12
DOI: 10.2312/GFZ.b103-99127

as accurately as possible.

The *determination of the poloidal magnetic field* in the mantle requires the solution of a parabolic partial differential equation, which is derived from the vectorial induction equation. The necessary boundary conditions are connected with magnetic observations on the earth surface. Traditionally, this problem is studied for a prescribed profile of the electric mantle conductivity and assuming a periodically oscillating field on the earth surface. The assumption of periodic behaviour replaces the inital condition which is normally required in the solution of the parabolic differential equation. If fields with non-restricted time-behaviour are to be studied, then a full initial-boundary value problem has to be solved, i.e. the initial condition may not be dropped. However, the determination of the poloidal magnetic field is not a standard initial-boundary value problem as there are only data observed on one boundary (earth surface), but not on any other interior surface like the CMB. Therefore, this task can be classified as an *inverse boundary value problem* for a parabolic partial differential equation. (From other points of view it is also synonymously addressed as non-characteristic Cauchy problem or non-harmonic downward field continuation, respectively.) In contrast to this problem, the term "*forward problem*" is used if a standard boundary value problem is given, i.e. input data on both boundaries are assumed to be known.

For a simple radial dependence of the mantle conductivity, $\sigma_M \sim r^{-\alpha}$, and a prescribed time dependence (e.g. periodic) of the magnetic field, analytical solutions of the forward problem were given, e.g., by McDonald (1957) and Smylie (1965). Instead of analytical methods, numerical methods are also be applied in the forward problem if the distribution of the conductivity is more complicated, e.g., as given by Rikitake (1973) and Shankland, Peyronneau & Poirier (1993).

Investigations and solutions related to the inverse boundary value problem (the downward continuation of the poloidal magnetic field) are involved in those methods which were developed for the calculation of electromagnetic core-mantle coupling torques or fluid outer core motions from magnetic surface data. For calculating the field on the CMB which enters into in the coupling torques mainly a perturbation method was applied. It replaces the unknown time derivative by a given time function. The unperturbed field is then the time variable geomagnetic potential field continued to the CMB, the perturbed field must be derived from the mantle induction equation according to the given time variations of the unperturbed field. The perturbation method is described, e.g., by Braginsky & Fishman (1977) and Benton & Whaler (1983). Greiner-Mai (1987, 1993, 1995) has continued these investigations with special emphasis on the consistency of the electromagnetic core-mantle coupling with ΔLOD for particular periods (e.g. the nearly 30-year period). Other authors - Gubbins & Bloxham (1985), Bloxham &

Scientific Technical Report STR 99/12
DOI: 10.2312/GFZ.b103-99127

Gubbins (1986), Bloxham (1989), Bloxham & Jackson (1992) and Holme (1998) - who use the potential (harmonic) downward continuation, gave CMB-fields solutions partly combined with fluid outer core motion determinations using, e.g., a stochastic inversion procedure. Voorhies & Nishihama (1994) considered different conductivity models and searched for common least squares solutions for the magnetic field and the velocity in the fluid outer core.

Because of the fact that the inverse boundary value problem is severely ill-posed, the theoretical and numerical *instability* should be taken into account in any case. Therefore, considering the noise of the data and its spectral structure the selection of a regularization strategy is necessary which forms the basis for a stable solution procedure. In this connection the close analogy with the inverse heat conduction problem (in the mathematical literature often referred to as the non-characteristic Cauchy problem) is helpful. Some approaches and numerous results can be found, e.g. in Dinh Nho Hào & Gorenflo (1991) and Reinhardt & Seifarth (1993).

Besides the geophysical implications of the problems addressed here, the comprehensive mathematical aspects are of interest. These have been studied intensively since the end of the fifties particularly in terms of the inverse heat conduction problem and semi-conductor or other material research important, e.g., for heat effects on spacecraft or in steel production. A common problem in geosciences is the problem of field continuation. It includes not only the determination of the poloidal magnetic field in the lower mantle and on the core-mantle boundary but also such problems as the geodetic boundary value problem, the downward continuation of the gravity field, the analogous problems for the static geomagnetic field and also geothermal problems. Common to all these problems is the instability due to the compactness ("smoothing property") of the ruling integral operator. A unifying mathematical view of these problems is provided by modern mathematical frameworks.

With respect to consistency, the problem of the core-mantle coupling appears as a multifold and coupled inverse problem which can be also understood as part of the *general inverse problem of the earth rotation* (Ballani 1987). The parameters of the coupling model are not prescribed but have to be estimated by comparison of the electromagnetic torques with those necessary to excite the observed ΔLOD. This inverse problem can only be solved stepwise by including additional information about the parameters of the model, e.g. from additional geophysical processes or from parameters estimated by laboratory experiments.

In this paper, one part of this general inverse problem, the non-harmonic downward continuation of the magnetic field to the CMB, is solved numerically.

On the basis of results found in the literature we develop an adapted solution procedure (for an outline see Ballani, Greiner-Mai & Stromeyer 1995) which bases

Scientific Technical Report STR 99/12
DOI: 10.2312/GFZ.b103-99127
Deutsches GeoForschungsZentrum GFZ

on an inversion approach in geothermics (Stromeyer 1983, 1984) and which includes some of the theoretical elements presented in, e.g. Eldén (1983). Some recent fundamental statements on stabilization are added.

After the introduction into basic physical and mathematical problems (sections 2.1 and 2.2) we give some insight into the theoretical properties of the non-harmonic downward continuation (section 3.1) and continue with the mathematically supported description of the numerical solution method (section 3.2). The method is applied to some models of conductivity connected with a supposed layering near the core-mantle boundary. The results are time series (one spherical harmonic mode) and the (5,5) radial field component of the poloidal field on the core-mantle boundary (section 4). The study concludes with a discussion of the properties of the procedure and the results obtained (section 5). In the appendices A and B an example for the analytical solution of the forward problem, and, connected with this, some remarks on the analytically formulated inverse problem are given.

Scientific Technical Report STR 99/12
DOI: 10.2312/GFZ.b103-99127

2. BASIC ASSUMPTIONS AND EQUATIONS

2.1 Basic model

First, the *mantle* is modelled by a rigid shell (figure 1) with the outer radius R_E (mean Earth radius) and the inner radius R_c (core radius).

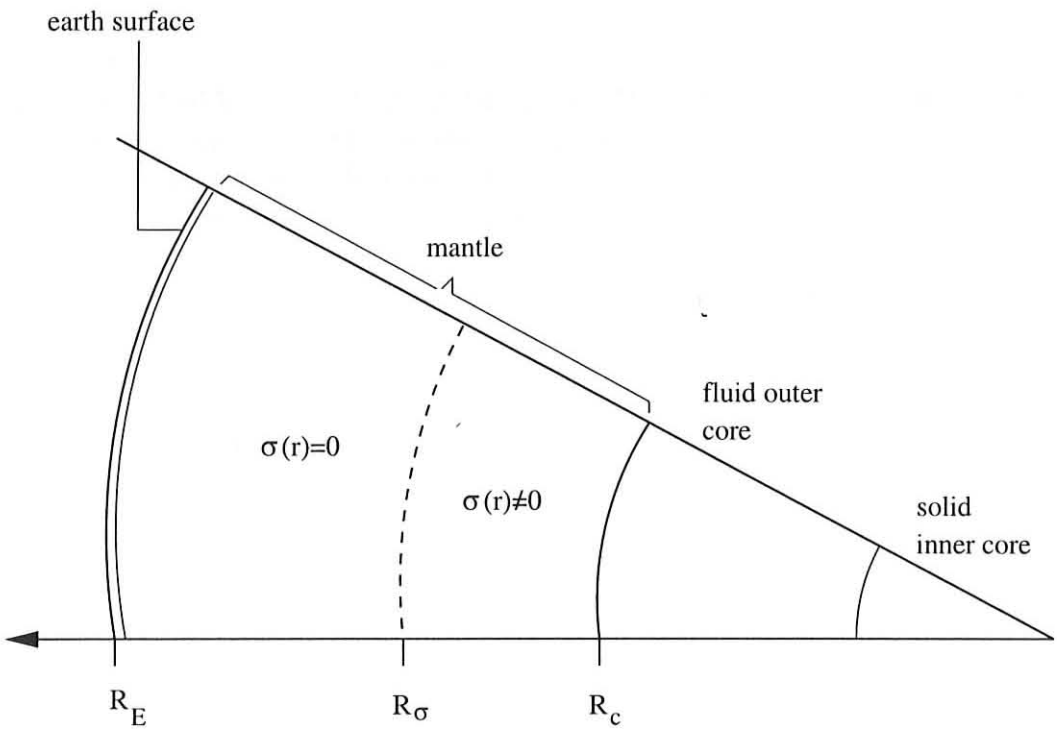

Figure 1: Geometrical assumptions in a spherically symmetric conducting earth model. $\sigma(r)$ is the electrical conductivity, $R_E = 6370\text{km}$, $R_\sigma = 5400\text{km}$, $R_c = 3400\text{km}$.

The *mantle conductivity*, $\sigma_M(r)$, is assumed to be a function of the radial distance r with $\sigma_M \neq 0$ for $R_c < r < R_\sigma$ and $\sigma_M = 0$ for $R_\sigma \leq r \leq R_E$. The two analytical dependencies on r considered for $R_c < r < R_\sigma$ are given by the semi-conductor formula and its first Taylor term, respectively

$$\sigma_M(r) = \sigma_0 \exp\left(-\alpha\left[\frac{r - R_c}{R_c}\right]\right), \tag{1}$$

$$\sigma_M(r) = \sigma_0 \left(\frac{R_c}{r}\right)^\alpha \quad , \tag{2}$$

Scientific Technical Report STR 99/12
DOI: 10.2312/GFZ.b103-99127
Deutsches GeoForschungsZentrum GFZ

where σ_0 is the mantle conductivity at the CMB ($r = R_c$) and α is the parameter determining the decrease of the conductivity with increasing distance from the CMB.

Crude bounds on the values of the parameters can be obtained from geomagnetic induction studies. Rotanova *et al.* (1985) used the 30- and 60-year periods of the secular variation to determine the parameters α and σ_0 in (1), and obtained values of α of about 6-8 and values of σ_0 between 1500 and 4000 Sm^{-1}. The parameter determining the magnitude of the electromagnetic torques is the ratio σ_0/α. According to Stix (1982) the ratio σ_0/α must be in the order of 100 Sm^{-1} for the electromagnetic coupling. He suggested that high values of both parameters α and σ_0 are optimal, i.e. models are prefered in which the mantle conductivity is concentrated in a thin shell near the CMB. Stix & Roberts (1984) and Greiner-Mai (1987, 1993) found that the magnitudes of the electromagnetic torques are consistent with LOD variations if σ_0 = 3000 S m^{-1} and $\alpha = 30$, i.e. $\sigma_0/\alpha = 100$. Greiner-Mai (1995) reduced the value of this ratio to about 30 by fitting the electromagnetic to the mechanical torques considering both the influence of the atmospheric excitation of ΔLOD and longer time series. However, the value of σ_M in the lower mantle is still under discussion (see also section 4.1).

Second, the *Earth's core* is assumed to be a "black box" in which the geomagnetic field is maintained by a dynamo process. The objective of our investigation is to determine the output of this "black box", i.e. the geomagnetic field at the CMB from observation at the Earth's surface. The penetration of the magnetic field through the mantle can be studied by forward methods for particular values of σ_0 and α.

Third, the solutions of the mantle induction equation are derived for the *poloidal magnetic field*, $\mathbf{B}_p$. This is the part of the magnetic field that can be observed outside the spherically symmetric conductor. The other part, the toroidal field is not considered in this paper. It can only be indirectly determined by a physical model of a process which involves the toroidal part, e.g. by comparison of the electromagnetic and mechanical torques derived from ΔLOD. Fortunately, the equations for the poloidal and toroidal parts are decoupled for a radially distributed mantle conductivity. We use the representation of the field by poloidal and toroidal *scalars*. Thus, the vector induction equations (3) and (4) shown in the next section can be transformed into two scalar equations, from which the poloidal induction equation is considered (for references see, e.g., Krause & Rädler 1980). The poloidal scalar field, S, is presented by a *spherical harmonic expansion*, whose associated coefficients, $S^{c,s}_{nm}(r, t)$, are called (poloidal) harmonic modes. The spectral range, considered here, comprehends the decadal time variations.

Scientific Technical Report STR 99/12
DOI: 10.2312/GFZ.b103-99127

2.2 Basic equations

The magnetic induction equations can be derived from the Maxwell equations by substituting for the current density and the electric field strength the magnetic flux density **B** and its time derivative, respectively. The vector induction equations are then given by

$$\begin{aligned} \text{curl}\ [(\mu_0\sigma_\text{M})^{-1}\text{curl}\ \mathbf{B}] &= -\dot{\mathbf{B}}\,, \quad \text{R}_\text{c} < \text{r} < \text{R}_\sigma, && (3)\\ \text{curl}\ \mathbf{B} &= 0\,, \quad \text{r} > \text{R}_\sigma, && (4)\\ \text{div}\ \mathbf{B} &= 0\,, \quad \forall\ \text{r}, && (5) \end{aligned}$$

where μ_0 is the permeability of free space. The boundary conditions at $\text{r} = \text{R}_\text{c}$, $\text{r} = \text{R}_\sigma$ and $\text{r} = \text{R}_\text{E}$ are the continuity of the flux density, $\mathbf{B}^+ = \mathbf{B}^-$, where the signs $+$ and $-$ denote the outer and inner side of the boundary, respectively. For spherical symmetry of σ_M and a solenoidal field ($\text{div}\,\mathbf{B} = 0$), the flux density can be decomposed orthogonally into toroidal and poloidal parts by

$$\mathbf{B} = \mathbf{B}_\text{t} + \mathbf{B}_\text{p} \qquad (6)$$

with

$$\begin{aligned} \mathbf{B}_\text{t} &= \text{curl}\,(\mathbf{r}\text{T}), && (7)\\ \mathbf{B}_\text{p} &= \text{curl curl}\,(\mathbf{r}\text{S}). && (8) \end{aligned}$$

The scalars are normed on the sphere by

$$\oiint \text{S}\,\text{d}\tilde{\omega} = 0 \quad \text{and} \quad \oiint \text{T}\,\text{d}\tilde{\omega} = 0\,, \qquad \text{d}\,\tilde{\omega} = \sin\vartheta\,\text{d}\vartheta\,\text{d}\varphi\ .$$

For the poloidal scalar S, the induction equations thus have the forms of the diffusion equation and the Laplace equation, respectively (see, e.g,, Krause & Rädler 1980):

$$\begin{aligned} (\mu_0\sigma_\text{M})^{-1}\Delta\text{S} &= \dot{\text{S}}\ , \quad \text{R}_\text{c} < \text{r} < \text{R}_\sigma && (9)\\ \Delta\text{S} &= 0\ , \quad \text{r} > \text{R}_\sigma\,, && (10) \end{aligned}$$

where Δ is the Laplace Operator. The boundary (interface) conditions are given by the continuity of S and its radial gradient according to the continuity of the radial component and the tangential components of the flux density, respectively (see eq.(15) below).
A setup for the scalar function S by means of spherical harmonics given by

$$\text{S} = \sum_{\text{n,m}} (\text{S}^\text{c}_\text{nm}(\text{r},\text{t})\cos\text{m}\varphi + \text{S}^\text{s}_\text{nm}(\text{r},\text{t})\sin\text{m}\varphi)\ \text{P}_\text{nm}(\cos\vartheta) \qquad (11)$$

Scientific Technical Report STR 99/12
DOI: 10.2312/GFZ.b103-99127

corresponds to a separation of the form $f(r,t) \cdot g(\vartheta,\varphi)$. Using the orthogonality of the spherical harmonics, we obtain from eqs. (9) and (10) the fully decoupled one-dimensional induction equations for the harmonic modes $S^{c,s}_{nm}(r,t)$:

$$D_n S^{c,s}_{nm} = \mu_0 \sigma_M \dot{S}^{c,s}_{nm} , \quad R_c < r < R_\sigma, \tag{12}$$

$$D_n S^{c,s}_{nm} = 0 , \quad r > R_\sigma , \tag{13}$$

where the operator D_n is defined by

$$D_n = \frac{\partial^2}{\partial r^2} + \frac{2}{r}\frac{\partial}{\partial r} - \frac{n(n+1)}{r^2}. \tag{14}$$

The interface conditions at $r = R_\sigma$ are

$$(S^{c,s}_{nm})^+ = (S^{c,s}_{nm})^-, \quad [\frac{\partial}{\partial r}\, rS^{c,s}_{nm}]^+ = [\frac{\partial}{\partial r}\, rS^{c,s}_{nm}]^-. \tag{15}$$

Eq. (13) is fulfilled with the usual potential solution for the field outside a conductor which is regular at infinity. From this solution the associated modes $C^{c,s}_{nm}(t)$ are defined by

$$S^{c,s}_{nm}(r,t) = C^{c,s}_{nm}(t)\, r^{-n-1}, \quad r \geq R_\sigma. \tag{16}$$

The geomagnetic potential V and its secular variation on the Earth's surface $r = R_E$ are derived from the scalar S by $V = -\frac{\partial}{\partial r}(rS)$. The geomagnetic potential is conventionally given as an expansion into spherical harmonics, whose coefficients are known as Gauss coefficients g_{nm} and h_{nm} (Mauersberger *et al.* 1959). Therefore, we obtain on the Earth's surface

$$C^c_{nm}(t) = \frac{1}{n}\, g_{nm}(t)\, \lambda_{nm}\, R_E^{n+2}, \qquad C^s_{nm}(t) = \frac{1}{n}\, h_{nm}(t) \lambda_{nm}\, R_E^{n+2}, \tag{17}$$

where λ_{nm} are the Schmidt's normalization coefficients defined by

$$\lambda_{nm} = \left((2 - \delta_{0m}) \frac{(n-m)!}{(n+m)!} \right)^{1/2} \tag{18}$$

with δ_{ik} Kronecker symbol. Solution (16) then determines the field outside the conducting part of the mantle in dependence of the Gauss coefficients, hereafter sometimes called data. The conventional harmonic downward continuation of the radial field component B_r can be obtained by substituting (16), (17) and (18) into (38) below (section 4.2).

It follows also from eq.(13) that the *secular variation field* can be obtained via the time derivatives, i.e. $\dot{S}^{c,s}_{nm} = \dot{C}^{c,s}_{nm}\, r^{-n-1}$ with $\dot{C}^{c,s}_{nm}$ calculated by the secular variation coefficients, $\dot{g}_{nm}$ and $\dot{h}_{nm}$, instead of the Gauss coefficients. Thus, the boundary values of the harmonic modes and their time derivatives at $r=R_\sigma$ can be derived from the solution (16) in dependence on the Gauss coefficients and their time derivatives as given in the literature.

Scientific Technical Report STR 99/12
DOI: 10.2312/GFZ.b103-99127

3. SOLUTION OF THE INVERSE BOUNDARY VALUE PROBLEM

3.1 Basic properties of inversion

Let us return to the scalar induction equation (9). It can be decomposed into decoupled one-dimensional parabolic partial differential equations (12) describing the diffusion of the harmonic modes $S_{nm}^{c,s}(r,t)$ of $S(r,t)$ through the electrically conducting spherical shell of the earth mantle. Dropping all subscripts and superscripts to simplify the notation (replacing $S_{nm}^{c,s} = u$) the inverse boundary value problem for the determination of $u(R_c,t)$ can be formulated as follows:

$$\frac{\partial^2 u}{\partial r^2} + \frac{2}{r}\frac{\partial u}{\partial r} - \frac{n(n+1)}{r^2}u = \mu_0 \sigma_M(r)\frac{\partial u}{\partial t} , \qquad R_c \le r \le R_\sigma , \quad 0 \le t \le T$$

with boundary conditions

$$u(R_\sigma,t) = \phi(t) ,$$
$$\frac{\partial u}{\partial r}(R_\sigma,t) + \frac{n+1}{R_\sigma}u(R_\sigma,t) = 0 \qquad (19)$$

and an initial condition

$$u(r,0) = \psi(r) .$$

The first boundary condition is directly connected with the geomagnetic data on the earth surface, while the other one is derived by the second continuity condition in (15) applied to the transition between the non-conducting and conducting mantle shell. The boundary values in (19) are given only on one side of the radial interval in contrast to the stable (properly posed) standard two-side boundary-value problems. There is a slight difference between the heat or diffusion problem and our case concerning the position of the temporally and/or spatially variable coefficient functions in the differential equation. However, this is only of numerical importance as long as extreme situations (nearly vanishing or unbounded coefficient functions) can be avoided. Modern theory for the inverse heat conduction problem provides results which allow wide classes of coefficient functions with only weak assumptions. The rigorous mathematical study of the considered inverse problem (19) requires its embedding into well defined function spaces. With appropriate specifications of those spaces, statements on correctness, i.e. *existence*, *uniqueness* and *stability* can be derived. The first two points can be usually satisfied (e.g., Tsutsumi 1965, Knabner & Vessella 1987, Dinh Nho Hào 1995).

Scientific Technical Report STR 99/12
DOI: 10.2312/GFZ.b103-99127

The *instability* of the problem has to be considered in greater detail. This is because several aspects are involved: data spacing, spectral contents, data errors, theoretical stability estimates and reconstruction behaviour, numerical-algorithmic processing and geophysical constraints. The main two reasons for the instability can be seen better if the inverse problem in the formulation (19) is transformed into a Volterra integral equation of the first kind (see (33) and (34) below): First, the compact integral operator has smoothing properties. Second, the unknown function cannot be reconstructed for time points near the end of the time interval (effect of convolution property). Third, some direct influence on the instability comes from the effect of the magnitude of the electrical conductivity as a coefficient function in the differential equation. The spectral aspect of the instability, i.e. the increasing amplitude of periodic parts is discussed below in appendix B.

Stable inversion can be forced mainly by means of constraints on the solution set. There are two possibilities which are studied here: *Stability estimates* and *Tikhonov regularization.*

A *stability estimate* describes the influence of the error bound ϵ of the data $\phi(t)$ (here the boundary values)

$$\|\phi\|_\beta \leq \epsilon$$

and an a priori bound E for the solution u

$$\|u\|_\gamma \leq E$$

on the solution of the inverse problem by means of an estimate of the following type:

$$\|\mathrm{u}\|_\alpha \leq \mathrm{C}\ \mathrm{f}(\epsilon, \mathrm{E})\ . \tag{20}$$

The effect of the bound E is a selection of solutions, for which the stability estimate directly represents the local continuity of the inverse operator. In the case of linearity, the function u appearing in this estimate (20) can also be replaced by *differences* of functions, so that the estimate can also be interpreted as the effect of the data error (exact data minus real data) on the disturbance (or error) of the solution (exact solution minus disturbed solution). These stability estimates can be found in the literature derived for the different situations: the function intervals considered (finite, half-infinite, infinite), the type of smoothness of the coefficients in the differential equation and the various norms or seminorms which reflect the smoothness of the solution itself.

Because the assumed conductivity models to be tested cover a wide range of magnitudes and are presented by different function types, their influence as a coefficient in the induction equation with respect to stability should be checked first

Scientific Technical Report STR 99/12
DOI: 10.2312/GFZ.b103-99127

theoretically. Let us briefly outline a general stability result from the literature (Knabner & Vessella 1988):

For the partial differential equation

$$a(x)\frac{\partial^2 u}{\partial x^2} + b(x)\frac{\partial u}{\partial x} + c(x)u = \frac{\partial u}{\partial t}, \quad 0 \le x < L, \quad t \ge 0 \tag{21}$$

having sufficiently smooth coefficients a(x), b(x), c(x), $c(x) \le 0$,
with boundary conditions $u(0,t) = \phi(t)$, $\frac{\partial}{\partial x}u(0,t) = 0$, $t \ge 0$,
and the assumptions $\|\phi\|_2 \le \epsilon$ (data) and $\|u(L,.)\|_2 \le E$ (solution),
and with the abbreviation

$$A(x) := \int_0^x a(s)^{-1/2}\,ds$$

the stability estimate of Hölder type

$$\|u(x,.)\|_2 \le C\,\epsilon^{1-A(x)/A(L)}(\epsilon^{A(x)/A(L)} + E^{A(x)/A(L)}), \quad 0 \le x < L, \quad C > 0 \tag{22}$$

can be derived.

Because (19) is a special case of eq.(21) we find from (22) after some simple calculations

$$A(r) = \int_{R_\sigma}^{r} (\mu_0 \sigma_M(r))^{1/2}\,dr, \quad R_c \le r \le R_\sigma. \tag{23}$$

Thus, (23) and (22) describe the influence of the electrical conductivity σ on the error behaviour in the interior of the radial interval.

It is also of some interest that the assumption on the smoothness of the "leading" coefficient a(x) can be considerably relaxed without changing the validity of the estimate. Therefore very general bounded functions, including step functions for the conductivity function $\sigma(r)$ are allowed. Stability estimations even exist, if a(x) is only approximatively known. A further important point is: Only this leading coefficient of the differential equation (21) has to be considered as an exponent for the bounds E and ϵ in the Hölder type estimation.

It is important to mention that there exists one exception of the validity of (22): the (right) inner point L of the radial interval corresponding to R_c is excluded, which is just of prime interest for our problem. To get stability estimates there at all, stronger bounds on the solution in this point are necessary. These are given by bounded radial or temporal derivatives of the function $u(r,t)$. In every case (with bounded radial and bounded time derivatives) the resulting estimate is no longer of the Hölder type but of the much weaker logarithmic type.

Scientific Technical Report STR 99/12
DOI: 10.2312/GFZ.b103-99127

Stability estimates using a bound for the *radial derivative* $\frac{\partial u}{\partial r}(r,t) \leq E$ can be found in (Knabner & Vessella 1987). However, the radial function behaviour cannot be accounted for in our approach because the input and output in the integral equation are pure time functions. From a physical point of view (smoothness constraints on the radial derivative of the unknown function on the core-mantle boundary), it may even be reasonable, to construct an algorithm working with the derivative of the function instead of the unknown function itself.

The problem of bounding the *temporal* behaviour of the solution on the core-mantle boundary by using different degrees and types of *derivatives* to get stability estimates (e.g. Engl & Manselli 1989; Manselli & Vessella 1991) directly corresponds to our integral equation approach. However, as the time function to be determined exists at the lower bound R_c of the radial interval, as mentioned, the stability estimates which can be reached are of much poorer quality than for any interior point of the radial interval. To demonstrate the characteristic features, we give two examples with different norms for the a priori bounds and for the stability estimate:

(1) The following general theorem (Manselli & Vessella 1991) shows clearly this logarithmic estimate under relatively weak assumptions on the function u and the coefficients of the partial differential equation, which in our application are only needed as radially variable functions (19).

Theorem:

Let u be a solution of the parabolic equation

$$\frac{\partial^2 u}{\partial x^2} = a(x,t)\frac{\partial u}{\partial t} + b(x,t)\frac{\partial u}{\partial x} + c(x,t)u \tag{24}$$

with $(x,t) \in Q := [0,L]\times[0,T]$ and $a, b, c, \frac{\partial a}{\partial t}, \frac{\partial b}{\partial x}$ bounded functions in Q.

We assume that for $\epsilon > 0$ $|u(0,t)| \leq \epsilon$ and $|\frac{\partial u}{\partial x}(0,t)| \leq L^{-1}\epsilon$ are satisfied

and, with the a priori bound $E > 0$,

$$\max_Q |u| + T^\theta \sup_{t_1 \neq t_2} \frac{|u(L,t_2) - u(L,t_1)|}{|t_2 - t_1|^\theta} \leq E \quad \text{is fulfilled for some} \quad \theta \in (0,1).$$

Then, for a fixed $\tau \in (0, 2/3\theta)$, there exists a constant ϵ_1 such that the estimate

$$|u(L,t)| \leq |\log \epsilon|^{-\tau} \quad \text{holds if} \quad \epsilon \leq \epsilon_1. \tag{25}$$

Scientific Technical Report STR 99/12
DOI: 10.2312/GFZ.b103-99127

(2) For the problem with the simpler differential equation

$$\frac{\partial^2 u}{\partial x^2} = \frac{\partial u}{\partial t}, \quad 0 \le x < 1, \quad \frac{\partial u}{\partial x}(0,t) = 0, \quad t \in R, \tag{26}$$

with $u(0,t) = g(t)$ given and $u(1,t) = f(t)$ unknown,
the L_2 norm-bounds for the data $\|g\|_2 < \epsilon$ and the solution $\|f\|_2 + \|\frac{\partial f}{\partial t}\|_2 < E$ respectively, yields the following result (Engl & Manselli 1989) :
For $n > 2$, there exist numbers K_n, with $\lim_{n\to\infty} K_n = \infty$, and exponents β_n with $\lim_{n\to\infty} \beta_n = 0$ such that the estimate

$$|f(t)| \le K_n \frac{E}{\left(\log \frac{E}{\epsilon}\right)^{1/4-\beta_n}}, \quad 0 \le t \le T \tag{27}$$

holds.

These logarithmic estimates show that the data error ϵ (or the difference between exact and disturbed data) can be estimated for the corresponding solutions within the order $O(1/\log(1/\epsilon))$. However, the constants involved are difficult to calculate, the influence of the coefficient functions of the differential equation (e.g. the electrical conductivity) can no longer seen explicitely as in the Hölder estimates given above, and they only provide a very raw error budget valid near the interval end.

The other possibility for a stable inversion, applied here, is the method of *Tikhonov regularization*. The principle of regularization is to change the mapping from the data to the solution from an operator of first kind to a more stable operator of second kind, i.e., the problem itself is changed to enable a controlled inversion.

Fundamental results on regularization with many details are published, e.g. in Plato (1995), Engl, Hanke & Neubauer (1996) and Hansen (1992, 1998).

The method of Tikhonov regularization, which is applied here (in a specific Tikhonov-Phillips variant, see section 3.2) to find solutions in a constraint solution set, consists in constructing a solution f by weighted minimization of the following quantity via a suitable choice of the parameter λ

$$\|Af_\lambda - \phi\|_\alpha + \lambda^2 \|L(f_\lambda - f^*)\|_\beta. \tag{28}$$

The norms $\|.\|_\alpha$ or seminorms $\|.\|_\beta$ and the smoothing functional L have to be specified. While the first term in (28) measures the data approximation at R_σ the second term accounts for the smoothness of the solution at R_c. The quantity f^* means an initial guess.

Scientific Technical Report STR 99/12
DOI: 10.2312/GFZ.b103-99127
Deutsches GeoForschungsZentrum GFZ

We do not use the regularization in this general form in our procedure. There are other regularization variants that are nearly equivalent to (28) (e.g. Hansen 1992,1998). From these we use that type which accounts especially for the data error:

$$\min\|L(f_\lambda - f^*)\|_\beta \quad \text{subject to} \quad \|Af_\lambda - \phi\|_\alpha = \epsilon. \tag{29}$$

Thus, a value of f_λ with optimal smoothness on the core-mantle boundary must be found approximating the data within a fixed error range.

In order to have a criterion for the regularized solutions, the so-called L-curve analysis, measuring the typical trade-off between solution smoothness and the degree of approximation to the data, is applied: The two contributions to the error parts, i.e. the approximation to the data and the degree of smoothness of the solution, have to be balanced.

The regularization method provides convergence even on weaker assumptions than those imposed for stability estimations discussed above. To prove and to reach convergence, some smoothness assumptions and bounds (specified below) combined with adapted parameter choice strategies are also necessary.

There are some useful results for our problem which take into account bounds on $\dot{f}$ and $\ddot{f}$, where $\dot{f}$ means the time derivative of f. Engl & Manselli (1989) show, that for the non-characteristic Cauchy problem (26) and for different degrees of smoothness for the solution $f(t)$, its reconstruction from noisy data g_ϵ, $\|g - g_\epsilon\| \leq \epsilon$, is possible with a reconstruction error which depends Hölder-continuously on the data error ϵ. The exponents between $1/2$ and $2/3$ depend on the smoothness assumed for the solution.

The results are L_2 convergence

$$\lambda(\epsilon) \sim \epsilon ... \epsilon^{2/3}: \quad \|f_{\lambda(\epsilon)} - f\|_{L_2} = o(\epsilon^{1/2}) ... O(\epsilon^{2/3}) \tag{30}$$

and uniform convergence

$$\lambda(\epsilon) \sim \epsilon ... \epsilon^{2/3}: \quad |f_{\lambda(\epsilon)}(t) - f(t)| = o(\epsilon^{1/2}) ... O(\epsilon^{2/3}), \quad 0 \leq t \leq T\,. \tag{31}$$

For the derivative $\dot{f}$, there was also L_2 convergence found. If the second term in (28), responsible for the smoothness of f, is chosen as pure L_2 norm without any further smoothness assumption for $f_{\lambda(\epsilon)}$, L_2 convergence can still be proved, but no longer pointwise convergence and convergence of the derivatives. These results refine and enlarge the logarithmic stability estimates shown above.

In the inverse problem (19), an *initial condition* $u(r,0) = \psi(r)$ has been included. This is, however, not necessary for a sufficient amount of data or in other special cases. Then this condition may be dropped (Dinh Nho Hào 1995; Reinhardt

Scientific Technical Report STR 99/12
DOI: 10.2312/GFZ.b103-99127

& Seiffarth 1993). In general, the initial condition is a weak point in the solution procedure because it introduces some degree of arbitrariness whose effect is strongest at the beginning of the reconstruction time interval.

Regarding the mathematical assumptions it should be kept in mind that these assumptions should be supplemented by physical constraints consistent with the degrees of freedom of the mathematical problem.

A practical aspect is that the measured data are always finite and discrete. For them, all function norms are equivalent and thus arbitrary estimates between these norms with suitable constants are possible. However, theoretical considerations of the continuous case, as given here for stability estimates and regularization, are nevertheless justified to guarantee stability in the limiting case: the density of the data can increase and more and more disturbing higher frequencies can be caused by uncontrolled noise.

3.2 Construction of the solving algorithm

Recently, for the solution of unstable non-characteristic Cauchy problems, several regularizing procedures have been developed and applied: Mollification, hyperbolic regularization, solution of integral equations of the first kind, variational methods and sequential regularization (for overviews see, e.g., Dinh Nho Hào & Gorenflo 1991 and Reinhardt & Seiffarth 1993).

We have constructed a method which combines elements of two of these procedures: We study the inverse problem for the differential equation (19) in the equivalent form of a Volterra integral equation of the first kind and solve an optimal control problem (a variational method) for the unknown boundary function ("boundary control"):
The quantity $\|\phi(.) - \mathrm{u}(\mathrm{R}_\sigma, .)\|$ is minimized, where u is the solution of (19).
$\|.\|$ is any fixed norm. $\phi(t)$, $0 \leq t \leq T$, is the boundary function which is known on R_σ. The unknown boundary function $\mathrm{u}(\mathrm{R_c}, .)$ is considered as the control.

The *algorithm* starts with a shifting standard transform for (19): A stable boundary value problem is solved so that $\psi(\mathrm{r}) \equiv 0$ (initial condition) is fulfilled.
Having modified the problem in this way, we want to specify the existing linear relationship

$$\mathrm{A}: \quad \phi \quad \Longrightarrow \quad \mathrm{f} \tag{32}$$

between the known boundary data function $\phi(.)$ on R_σ and the unknown function $\mathrm{f}(.) := \mathrm{u}(\mathrm{R_c}, .)$ on $\mathrm{R_c}$.

Scientific Technical Report STR 99/12
DOI: 10.2312/GFZ.b103-99127

Only for very simple cases (e.g. $\sigma_M(r) = \text{const.}$) the kernel $k(\tau)$ in (33) below can be directly determined from the differential equation via an integral (e.g. Laplace) transform technique. Then, the Volterra integral equation of the first kind

$$\phi(t) = \int_0^t k(t-\tau)\, f(\tau) d\tau \tag{33}$$

can be obtained in explicit form. The convolution kernel $k(t)$ is analytically known and can be described by an infinite series (Eldén 1983).

However, in our case with $\sigma_M(r) \neq \text{const.}$, i.e. for a partial differential equation with locally variable coefficients, the situation is more difficult. We know only that the corresponding relation is still given by an *abstract* linear operator equation of the first kind

$$\phi = A\, f, \qquad A \text{ Volterra integral operator,} \tag{34}$$

but we cannot specify the kernel explicitely. However, it is known that this type of operator can be replaced by a finite dimensional approximation. Thus, we introduce a time discretization $\{t = t_i, i = 1, N\}$ and approximate the unknown boundary function $f(t)$ by an appropriate set of base functions $e_k(t)$:

$$f(t) \approx \sum_{k=1}^{N} f_k\, e_k(t). \tag{35}$$

These steps contain some degree of freedom to account for physical constraints and also to restrict the resolution and to coarsen the final time discretization. Without loss of generality we adopt the simplest choice for the base functions:
$e_k(t_i) = \delta_{ki}$. Then a matrix (a_{ik}) describing the linear relationship and approximating the operator A in (34) can be determined in the following way: With the boundary functions

$$\frac{\partial u^k}{\partial r}(R_\sigma, t) + \frac{n+1}{R_\sigma} u^k(R_\sigma, t) = 0\,, \qquad u^k(R_c, t) = e_k(t)\,, \quad k = 1, \ldots, N, \tag{36}$$

a stable solution of the differential equation (19) can be found. This determines the kth column of (a_{ik}), so that the whole matrix is given by

$$(a_{ik}) = u^k(R_\sigma, t_i), \quad i = 1, \ldots, N, \quad k = 1, \ldots, N. \tag{37}$$

Because of its Toeplitz structure due to the convolution kernel, it is only necessary to calculate the first matrix column ($k = 1$). The other ones ($k = 2, \ldots, N$) then are generated by shifting their elements downward iteratively, which results in the known triangular matrix structure. The implementation of this step thus requires only the numerical solution of one stable problem for the first matrix column.

Scientific Technical Report STR 99/12
DOI: 10.2312/GFZ.b103-99127

Having the matrix (a_{ik}) determined, the regularization procedure (the boundary control process) can be started. For our purposes, it is the proper inversion procedure with some degrees of freedom left which may be used to account for the geomagnetic aspects of the problem. The inversion algorithm is based partly on some tools found in (Hansen 1992,1998) connected with the theory described in section 3.1. Thus, our approach can be adapted to the special problem considered. The algorithm ends with a standard transform which restores the original initial condition.

Scientific Technical Report STR 99/12
DOI: 10.2312/GFZ.b103-99127

4. RESULTS

4.1 Used magnetic data and electrical conductivity models

The magnetic input data given on the earth surface are the Gauss coefficients g_{nm}, h_{nm} of the geomagnetic potential field (see eq. (17)). With the geomagnetic potential V (section 2.2) given on the earth surface, the link to our parabolic differential equation is given via eq. (16). By this relation, the scalar quantities and the radial derivatives in (15) for R_σ, which are necessary for the boundary conditions $\phi(t)$ in (19), can simply be calculated by means of the Gauss coefficients.

A comparison between the Gauss coefficients for the time interval beginning in 1550, which were determined by different authors, is given, e.g. by Mauersberger (1952). But for the downward continuation we use time series beginning in 1900 for reasons of accuracy. Before this date, there are too many contradictions between the time series proposed by different authors. In addition, because of non-regular and wide spacing, it is impossible to get significant spectral estimates. As an example of the situation, the Gauss coefficient $h_{11}(t)$ is shown in figure 2 (see next page). The time span comprehends the whole measuring period and that interval which starts at the beginning of this century which is used for our calculations.

The series after 1900 were calculated by an integration procedure from the secular variation coefficients of Hodder (1981) so that two year spaced series from 1903 to 1975 resulted. These time series were extended by IGRF (International Geomagnetic Reference Field) values until 1987 giving data at 43 time points totally. By using these series, periods between about 10 years and slightly more than 30 years can be estimated. For the study of the 60 to 80-year periods, the series should be longer by about 50 years.

Another aspect of the data to be addressed here concerns their errors, which are difficult to estimate. Comparing different references it is reasonable to assume that there is a monotonous decrease of errors (perhaps from about 100 nT down to 10 nT) for the interval from 1903 until 1987. This order of magnitude (the decrease by a factor of 10) can also be found for the Gauss coeficcient g_{01} in (Bloxham & Jackson 1992). The incompletely known error of the data on the earth surface is the most important reason for the necessity of studying stability estimates and stabilizing the solution by a regularization process.

The *electrical conductivity* of the mantle as prescribed input quantity in our algorithm is, especially for the lower mantle, not well known and a subject of continued discussion. The traditional analytic forms (power law or exponential law

Scientific Technical Report STR 99/12
DOI: 10.2312/GFZ.b103-99127

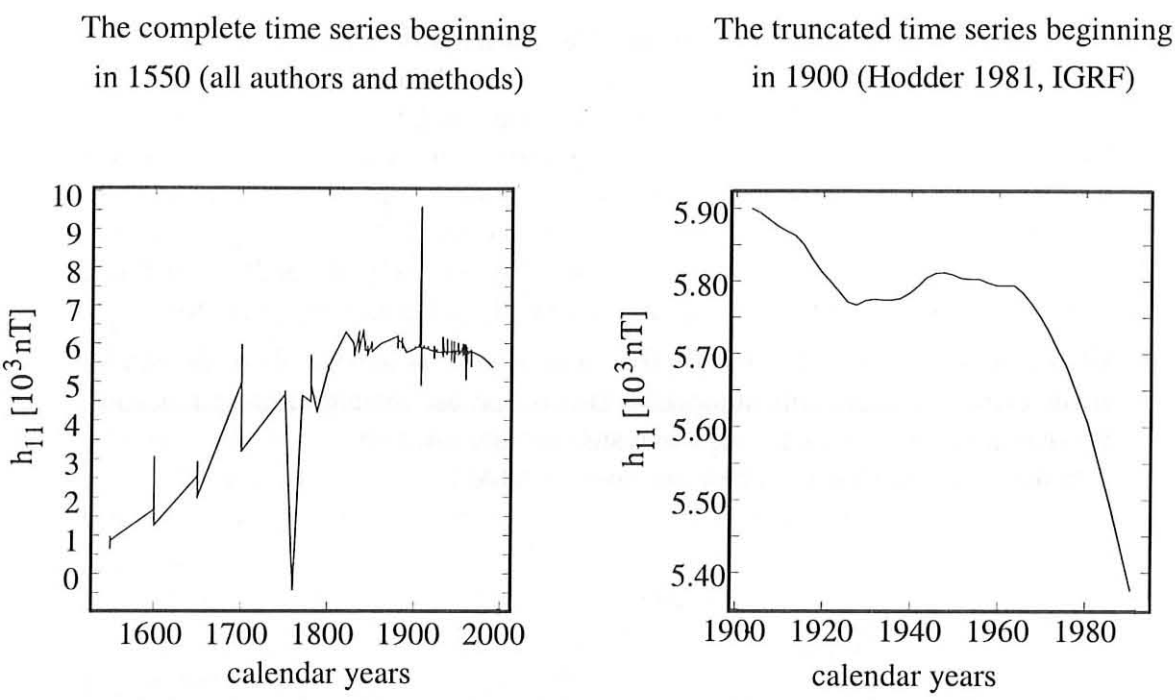

Figure 2: Example of a magnetic data time series: The Gauss coefficient $h_{11}(t)$ of the spherical harmonic expansion of the geomagnetic potential field (left diagramme: all values available according to Barraclough (1978), Hodder (1981), IGRF).

formulae, cf. eqs. (1) and (2)) are largely consistent with the deep earth interior material investigations (semi-conductor property of the material, high-pressure experiments). During the last decade, the studies resulted in curves monotonically increasing with depth in the mantle and ending with values of only some Sm^{-1} at the core-mantle boundary (e.g. Poirier & Le Mouël 1992; Shankland, Peyronneau & Poirier 1993). But with these values, the electromagnetic coupling torques are not sufficiently high (e.g., Holme 1998). However, the D" layer at the bottom of the mantle supposedly consisting of core-infiltrated material with about 100 km to 200 km in thickness and a conductivity of up to 4000 Sm^{-1} could generate the lacking torque. This layered conductivity can be modelled by a step function. Of significance to our study is also the large range of magnitudes of the assumed mantle conductivity. This is one reason for some destabilizing influence on the numerical solution of the inverse boundary value problem which exists in addition to the inherent theoretical instability. One advantage of the numerical algorithm used is the possibility to work with arbitrary conductivity distributions. In particular, there is no problem with (bounded) radial discontinuities. Thus, our algorithm agrees with the theoretical assumptions and estimates which guarantee

Scientific Technical Report STR 99/12
DOI: 10.2312/GFZ.b103-99127
Deutsches GeoForschungsZentrum GFZ

stability for a wide range of coefficient types in the differential equation. By this it is possible to study the effects of simply structured conductivity layers near the core-mantle boundary. An interesting additional application, to study the effectiveness of our downward continuation algorithm, concerns the field behaviour in a proposed *passive upper core layer* in the fluid outer core which is locked to the mantle and in which the conductivity jumps into the 10^5 Sm^{-1} range (see, e.g., Lister & Buffett 1998). This causes an instability (severely ill-conditioned matrix in the algorithm, see next section) which is nearly out of numerical control.

Of course, also the non-conducting (harmonic) case $\sigma_M \equiv 0$ should be favourably treated with the stabilizing algorithm. This is because the algorithm can account for the influence of the data noise and stabilize the solution.
The partial σ_{M} models used here are given in table 1.

Conductivity Model 1			
upper mantle	main lower mantle	lower mantle's D" layer	passive upper core layer
$r > R_\sigma$	$R_c + 200\,\mathrm{km} < r \leq R_\sigma$	$R_c \leq r \leq R_c + 200\,\mathrm{km}$	$R_c - 50\,\mathrm{km} \leq r < R_c$
$\sigma_M = 0$	$\sigma_{M_1}(r) = 10\,\mathrm{Sm}^{-1}(\frac{R_c}{r})^5$	$\sigma_{M_1}(r) = 3 \times 10^3\,\mathrm{Sm}^{-1}$	$\sigma_{pul}(r) = 2 \times 10^5\,\mathrm{Sm}^{-1}$
Conductivity Model 2			
$r > R_\sigma$	$R_c + 3\mathrm{km} < r \leq R_\sigma$	$R_c \leq r \leq R_c + 3\mathrm{km}$	$R_c - 50\mathrm{km} \leq r < R_c$
$\sigma_M = 0$	$\sigma_{M_2}(r) = 10\,\mathrm{Sm}^{-1}(\frac{R_c}{r})^5$	$\sigma_{M_2}(r) = 2 \times 10^5\,\mathrm{Sm}^{-1}$	$\sigma_{pul}(r) = 2 \times 10^5\,\mathrm{Sm}^{-1}$
Conductivity Model 3			
$\sigma_M = 0$	$\sigma_M = 0$	$\sigma_M = 0$	———

Table 1: Models of the mantle conductivity $\sigma_{\mathrm{M}}(r)$ used for numerical calculations, $R_\sigma = 5400$ km and $R_c = 3400$ km. The fields are calculated at the CMB and at the bottom of the passive upper core layer, respectively and are compared with the harmonic downward continuation (Model 3).

Scientific Technical Report STR 99/12
DOI: 10.2312/GFZ.b103-99127

4.2 Downward continuation of magnetic field components

In this section we consider how the downward continuation algorithm works, which modifications and criteria are possible and which mathematical or numerical features are obtained. As our "model" component and boundary function $\phi(t)$ in (19) we choose the data function $h_{11}(t)$ (Gauss coefficient) from the spherical harmonic expansion of the geomagnetic potential V at the earth surface. Curves for $h_{11}(t)$ are presented in figure 2. As has been mentioned in section 4.1 a homogeneous error evaluation for each time point of the data series does not exist. Thus, as a first estimation, the minimum amplification of errors can be obtained by looking at the harmonic downward continuation giving a factor of at least 13 for $n = 1$. For the non-harmonic downward continuation, an error with an oscillating behaviour would have to be estimated exponentially by means of the estimate (51) (Appendix B). However, this raw estimate is already sufficient to get some insight into the effect of the input data characteristics in the regularization procedure for our ill-posed inverse boundary value problem.

The set of base functions $e_k(t)$ for the boundary function (35) is specified by self-created triangle-like peak-functions to approximate the Kronecker symbol condition in the time points t_i. The numerical integration of the stable two-side boundary value problems with boundary conditions (36) to determine the Toeplitz matrix A in eq.(37) is implemented by the conventional Crank-Nicholson algorithm with a spacing for the radial interval of 0.2 km and time steps of 2 years corresponding to the data given.

For the regularization according to (29) the norms are taken as

$$\|u(R_c,.)\|_\alpha = \|u(R_c,.)\|_2 := \left(\int_0^T |u(R_c,t)|^2 \, dt \right)^{1/2}$$

and for $\|.\|_\beta$ the norms

$$\|u(R_c,.)\|_2 \qquad \text{and} \qquad \|u(R_c,.)\|_{W_2^1} := \|u(R_c,.)\|_2 + \|\frac{\partial u}{\partial t}(R_c,.)\|_2$$

are applied which is adapted to the results for the stability estimations and for the regularization. It should be pointed out that the derivative considered here in the regularization by means of the W_2^1 norm refers to the time variable and not to the spatial variable because the inversion approach constructed here applies only to time dependent functions.

The values of the different σ_M models and some other parameters are given in table 1. For the presentation of the results, we define the time functions h_{11}^{CMB} and

Scientific Technical Report STR 99/12
DOI: 10.2312/GFZ.b103-99127

h_{11}^{pul} as coefficient of the solution analogously to the harmonic continuation (16), (17) as

$$h_{11}^{CMB}(t) = \frac{1}{R_c} S_{11}^{s}(R_c, t) \quad \text{and} \quad h_{11}^{pul}(t) = \frac{1}{R_c - 50km} S_{11}^{s}(R_c - 50km, t) \,,$$

respectively.

The *resulting CMB-functions* can be seen in the figures 4, 6 and 8 showing different cases of the regularized, downward continued magnetic field component h_{11}^{CMB} and h_{11}^{pul} calculated with the different regularization norms. To emphasize the higher frequency structure and for better comparison, a linear trend was removed. Clearly, the typical smoothness behaviour of the different norms is observed, which, with a certain degree of freedom, can be selected corresponding to the physical background. As expected, the regularization with the weaker $\|.\|_2$ norm results in more oscillating solutions. For comparison the downward continuation is calculated also for the harmonic case ($\sigma_M(r) \equiv 0$), so that the influence of the presence of the mantle conductivity and of its distribution can be studied. In addition, the spectrally founded effect of amplitude amplification and phase shifting appear in the figures, especially compared with the harmonic downward continuation.

The solutions were calculated for *two depth levels*: First, the field is described on the core-mantle boundary. In addition, as an experiment, the downward continuation of the field component due to $h_{11}(t)$ is presented for a second level (50 km beneath the CMB) inside a supposed passive layer on top of the fluid outer core. As the core-mantle boundary solution for σ_{M_2} almost completely coincides with the harmonic continuation, it is not shown. Thus, the effect of this conductivity model at the deeper level ($R_c - 50km$) is mainly due to the conductivity $\sigma_{pul}(r)$. With greater depth and sufficiently high conductivity values the solution becomes stronger modulated.

The degree and the quality of the *data approximation at* R_σ in the residual norm $\|.\|_\alpha = \|.\|_2$ according to the first term in (28) is shown for each solution (figures 5, 7 and 9). Considering the assumed time-dependent errors of the h_{11}-data for the past, a compensatory matching 5% bound was fixed a priori.

At this point, it should be stressed that - concerning the significance of the solution - the *temporally middle section* of each solution submits the best information on the input data, the boundary values on the earth surface. The *beginning of the time interval* is dominated by the influence of the arbitrary initial condition which was taken here as the harmonic continuation. By means of the phase shift compared to the harmonically downward continued solution this time interval can be evaluated. The *final part of the time interval* is dominated by the regularization norm because

Scientific Technical Report STR 99/12
DOI: 10.2312/GFZ.b103-99127

the curve is forced to fulfill the corresponding minimum condition at the end of interval and for this time interval no longer significant to the data on the earth surface.

Moreover, for each regularized solution, the *trade-off* between solution smoothness at R_c and $R_c - 50\text{km}$ ("solution norm"), respectively, and the data approximation achieved on the R_σ level ("residual norm") is given using the "L-curves" (figures 10-13) (see Hansen 1992,1998). These are shown for the conductivity σ_{M_1} on both levels and generated by means of both stabilizing regularization norms. In each case the $\|.\|_2$ norm is used as residual norm measuring the data approximation at R_σ.

To characterize the properties and the limiting difficulties of the numerical procedure a further criterion may be called: The condition numbers of the regularization matrix A reach the order of 10^{14} at the core-mantle boundary for the σ_{M_1} solution and 10^{19}, especially in the higher conducting case of the passive upper core layer above the R_c-50 km level. It has to be mentioned that, with conductivity values greater than those selected here, the regularization process can no longer be numerically controlled.

In addition to the study of the temporal character of the non-harmonic downward continuation by means of a single Gauss coefficient, the spatial behaviour and the global effects can be demonstrated with the *radial component* B_r of the magnetic field covering locally spectral components of different degree and order. By means of the Gauss coefficients $g_{nm}(t)$ and $h_{nm}(t)$ as boundary values taken up to degree and order 5, the field component $B_r(r,t)$:

$$B_r = \frac{1}{r} \sum_{n,m} \left(S^c_{nm}(r,t)\cos m\varphi + S^s_{nm}(r,t)\sin m\varphi\right)\ n(n+1)\,P_{nm}(\cos\vartheta) \qquad (38)$$

was calculated at the core-mantle boundary $r = R_c$ for two time points - 1930 and 1960 - belonging to the middle part of the interval between 1903 and 1990 - and additionally for these time points at a depth of 50 km $r = R_c - 50\text{km}$ beneath the core-mantle boundary (see figures 14-17). As conductivity models σ_{M_1} and σ_{pul} (see table 1) were applied. Because of the differing data quality, it was necessary to control the regularization of each component individually. The solution presented here was calculated by means of regularization with the W_2^1 norm. The comparison of our results with published CMB fields from other authors which were calculated for nearly the same epochs should take into consideration that our computations include the influence of the conductivity from the mantle and partly also from the fluid outer core.

The properties of the time structure, which can be derived from the couples of figures 14, 15 and 16, 17, respectively, confirm the results discussed for the downward continuation of the single Gauss coefficient $h_{11}(t)$ (increasing temporarily

Scientific Technical Report STR 99/12
DOI: 10.2312/GFZ.b103-99127

modulation with depth, a kind of integral influence of the electrical conductivity, phase shifting and amplitude amplification). If we consider those figures which concern the same time point but present different depths (e.g. figures 14 and 16 for 1930) the anomalies with their spatial details can be seen better, especially those around the south pole and beneath Siberia. Analogous observations concerning the spatial structure can be also made for 1960 (figures 15 and 17). From these significant spatial modulations, it can be concluded that the velocity field in the top layer of the fluid outer core must have finer scales with increasing depth. Summarily, we find that highly conducting layers near the CMB can change the continuation results compared with the harmonic downward continuation considerably. This should have consequences for the physical quantities which are asociated with the magnetic field at the CMB.

Scientific Technical Report STR 99/12
DOI: 10.2312/GFZ.b103-99127

5. CONCLUDING REMARKS

The non-harmonic downward continuation of the magnetic field presented here has consequences in two fields of investigation:
(A) physical parameters associated with the magnetic field and
(B) the further development of the inverse theory accounting for the uncertainty of input data

Concerning (A) it is of high interest to know the magnetic field on the core-mantle boundary and in the earth lower mantle in the decadal time scale. One reason is the necessity to calculate the electromagnetic core-mantle coupling, with which the correlation between Earth rotation and magnetic field in this time scale can be explained. Our results suggest that computations of coupling torques by using the regularization method in the downward continuation process and a sufficiently high conductivity may lead to new aspects. In particular, the magnetic field on the CMB is used for the determination of the velocity fields in the fluid outer core (frozen-field theory) which plays an important role in the calculation of toroidal coupling torques. The results derived from the non-harmonic downward continuation procedure can be differ from those basing only on the harmonic downward continuation of the magnetic field components.

Concerning (B) this problem of downward continuation is itself an inverse problem and, at the same time, part of a joint coupled inverse problem: As a downward continuation problem it is connected with the assumptions on the conductivity model for the lower mantle. Because in our downward continuation problem data are given only on one side of the radial interval and because nonvanishing electrical conductivity in the lower mantle has been assumed, the corresponding mathematical problem can be characterized as an inverse boundary value problem which describes a non-harmonic downward continuation process. In this sense, the presented approach for the solution of this inverse problem can be seen in the continuity of papers by Benton & Whaler (1983) and Bloxham (1989), who used a perturbation method or a stochastic inversion approach, respectively. We have solved the problem more extensively applying more recent mathematical tools.

The formal identity with the inverse heat conduction problem (often also: non-characteristic Cauchy problem) has led us to the construction of a regularizing numerical algorithm for this severely unstable inverse problem. With this, it has become possible to account for arbitrary conductivity models, for the composition of the solving function by certain base functions ("boundary control approach") and for different solution strategies, i.e. the assumption of norm bounds on the solution to reach a certain type of smoothness or to account for the degree of approximation to the data. The instability of the problem is not only influenced by the conductivity function but also by the spectral content of the data. Especially

Scientific Technical Report STR 99/12
DOI: 10.2312/GFZ.b103-99127

because of the largely unknown noise of the older data - we use a nearly one-hundred year time span - stabilizing estimates are necessary. These estimates, given in the literature and adapted to our inverse problem, can be used to give Hölder type error estimates inside the lower mantle depending on the smoothness constraint adopted for the solution, an error estimate for the input data, and an exponent describing the integral influence of the conductivity function. The numerical construction of the time series of the magnetic field on the core-mantle boundary is achieved via a regularization procedure for which, dependent on the assumed smoothness of the solution connected with a parameter choice strategy for the minimization, also theoretical approximation error results of Hölder type exist. Because each regularization procedure - we apply a modification of the Tikhonov regularization - combined with special norms gives somewhat different results, only a "synoptic" view leads to an approximative impression on the solution behaviour. These aspects of instability and its regularization should also be taken into consideration if the harmonic downward continuation is to be applied.

To evaluate the physical results, the background of the diffusion equation should be kept in mind: Beyond of the question of smoothness, amplitude amplification and phase shifting, which can be seen in the examples (figures in section 4.2) the first and the last part of the reconstruction time interval should be excluded from the interpretation.
Under these aspects, the epochs (1930, 1960) of the radial component of the (5,5) core-mantle boundary field were selected (figures 14-17). This cutting of the time interval for a physically significant interpretation and the derivation of parameters of fluid matter velocity and coupling torques requires the search and the use for a longer span of the magnetic input data base.

The method can be adapted to other questions, e.g. the further investigation of the spectral characteristics or the field continuation into the upper layers of the fluid outer core. But this application of our formalism is limited by the numerical conditions. For reaching better error estimations of the magnetic field on the core-mantle boundary, it is neccessary to find more adequate time dependent error bars for the Gauss coefficients g_{nm} and h_{nm} for the beginning of the time interval and to have a theory which estimates the effect of time dependent errors on the construction of solutions of the unstable non-characteristic Cauchy problem.

Acknowledgements

We thank R. GORENFLO (Berlin), DINH NHO HÀO (Siegen, Hanoi), R. PLATO (Berlin) and T. J. SHANKLAND (Los Alamos (New Mexico), Bayreuth) for helpful discussions and J. GOTTLIEB (Karlsruhe, Fort Collins (Colorado)) for a critical review. The authors benefitted also from the support with some literature by S.

VESSELLA, (Florence). We are grateful to our colleagues EVA FELSMANN and HANS KÜHN for their technical help. D. WOLF has carefully checked the article. We thank him for useful hints and discussions.

REFERENCES

Backus, G. E., 1968. Kinematics of the geomagnetic secular variation in a perfectly conducting core, *Phil. Trans. R. Soc. Lond.*, **A263**, 239-266.

Ballani, L., 1987. Inverse Problems Concerning the Dynamics of the Earth's Rotation. In: Holota, P., (ed.): Proceedings of the International Symposium "Figure and Dynamics of the Earth, Moon, and Planets", Part III. Astronomical Institute of the Czechoslovak Academy of Sciences, Research Institute of Geodesy, Topography and Cartography, Prague, Czechoslovakia, pp. 851–878.

Ballani, L., Greiner-Mai, H. & Stromeyer, D., 1995. Über ein nichtcharakteristisches Cauchy-Problem bei der geomagnetischen Kern-Mantel-Kopplung, *ZAMM*, **75**, 613-614.

Barraclough, D. R., 1978. Spherical harmonic models of the geomagnetic field, Institute of Geological Sciences, *Geomagn. Bull.*, No. 8.

Benton, E. R. & Whaler, K. A., 1983. Rapid diffusion of the poloidal geomagnetic field through the weakly conducting mantle: a perturbation solution, *Geophys. J. R. astr. Soc.*, **75**, 77-100.

Bloxham, J., 1989. Simple models of fluid flow at the core surface derived from geomagnetic field models, *Geophys. J. Int.*, **99**, 173-182.

Bloxham, J. & Gubbins, D. , 1986. Geomagnetic field analysis, IV, Testing the frozen-flux hypothesis, *Geophys. J. R. astr. Soc.*, **84**, 139-152.

Bloxham, J. & Jackson, A. , 1992. Time-Dependent Mapping of the Magnetic Field at the Core-Mantle Boundary, *J. Geophys. Res.*, **97**, B13, 19,537-19,563.

Braginsky, S. I., 1984. Short-Period Geomagnetic Secular Variation, *Geophys. Astrophys. Fluid Dynamics*, **30**, 1-78.

Braginsky, S. I. & Fishman, V. M. , 1977. Screening of the Magnetic Field in the Mantle Under Electrical Conductivity Concentrated Close to the Core Boundary, *Geomag. Aeron.* **17**, 907. (in Russian)

Bullard, E. C., Freedman, C., Gellman, H. & Nixon, J., 1950. The westward drift of the Earth's magnetic field, *Phil. Trans. R. Soc. Lond.*, **A243**, 67-92.

Dinh Nho Hào, 1995. A Noncharacteristic Cauchy Problem for Linear Parabolic Equations I: Solvability. *Math. Nachr.* **171**, 177–206.

Scientific Technical Report STR 99/12
DOI: 10.2312/GFZ.b103-99127

Dinh Nho Hào, & Gorenflo, R., 1991. A noncharacteristic Cauchy problem for the heat equation. *Acta Appl. Math.* **24**, 1–27.

Eldén, L., 1983. The numerical solution of a non-characteristic Cauchy problem for a parabolic equation. In: Deuflhard, P., Hairer, E., (eds.): Numerical Treatment of Inverse Problems in Differential and Integral Equations. Birkhäuser, Boston, Basel, Stuttgart, pp. 246–268.

Engl, H. W. & Manselli, P., 1989. Stability estimates and regularization for an inverse heat conduction problem, *Numer. Funct. Anal. and Optimiz.*, **10**, 517-540.

Engl, H. W., Hanke, M. & Neubauer, A., 1996. Regularization of Inverse Problems, Kluwer Academic Publishers, Dordrecht/Boston/London.

Gire, C., & Le Mouël, J.-L., 1990. Tangentially geostrophic flow at the core-mantle boundary compatible with the observed geomagnetic secular variation: the large-scale component of the flow, *Phys. Earth. Planet. Int.*, **59**, 259-287.

Greiner-Mai, H., 1986. Theoretische Betrachtungen zum Verhalten des Magnetfeldes in einem sphärischen Erdmodell, *Astr. Nachr.*, **307**, 201-208.

Greiner-Mai, H., 1987. The influence of the electromagnetic core-mantle coupling torques on Earth's rotation, *Astr. Nachr.*, **308**, 17-26.

Greiner-Mai, H., 1993. Decade variations of the Earth's rotation and geomagnetic core-mantle coupling, *J. Geomag. Geoelectr.*, **45**, 1333-1345.

Greiner-Mai, H., 1995. About possible geophysical causes of the decade fluctuations in the length of day, *Astr. Nachr.*, **316**, 311-318.

Gubbins, D. & Bloxham, J., 1985. Geomagnetic field analysis,III, Magnetic fields on the core-mantle boundary, *Geophys. J. R. astr. Soc.*, **80**, 695-713.

Hansen, P. C., 1992,1998. Regularization Tools. A Matlab Package for Analysis and Solution of Discrete Ill-Posed Problems, Lyngby, Denmark, 109 pages.

Hinderer, J., Legros, H., Jault, D. & Le Mouël, J.-L., 1990. Core-mantle topographic torque: a spherical harmonic approach and implications for the excitation of the Earth's rotation by core motions, *Phys. Earth Planet. Inter.*, **59**, 329-341.

Hodder, B. M., 1981. Geomagnetic secular variation since 1901, *Geophys. J. R. astr. Soc.*, **65**, 763-776.

Holme, R., 1998. Electromagnetic core-mantle coupling-I. Explaining decadal changes in the length of day, *Geophys. J. Int.*, **132**, 167-180.

Jault, D. & Le Mouël, J.-L., 1990. Core-mantle boundary shape: constraints inferred from the pressure torque acting between the core and the mantle, *Geophys. J. Int.*, **101**, 233-241.

Scientific Technical Report STR 99/12
DOI: 10.2312/GFZ.b103-99127

Jochmann, H. & Greiner-Mai, H., 1996. Climate variations and the Earth's rotation, *J. Geodynamics*, **21**, 161-176.

Knabner, P. & Vessella, S., 1987. Stabilization of ill-posed Cauchy problems for parabolic equations, *Ann. Mat. Pura Appl.*, **CIL** IV, 393-409.

Knabner, P. & Vessella, S., 1988. The Optimal Stability Estimate for some Ill-posed Cauchy Problems for a Parabolic Equation. *Math. Methods in the Appl. Sci.*, **10**, 575-583.

Krause, F. & Rädler, K.-H., 1980. *Mean Field Magnetohydrodynamics and Dynamo Theory*, Akademie Verlag, Berlin.

Lambeck, K. & Cazenave, A., 1976. Long term variations in the length of day and climate change, *Geophys. J. R. astr. Soc.*, **46**, 555-573.

Le Mouël, J.-L., Hulot, G. & Poirier, J.-P., 1997. Core-Mantle Interactions, in: Earth's Deep Interior. The Doornbos Memorial Volume. Ed. by D. J. Crossley. Gordon & Breach Science Publ., Amsterdam, pp. 197-221.

Lister, J. R. & Buffett, B. A., 1998. Stratification of the outer core at the core-mantle boundary *Phys. Earth Planet. Inter.*, **105**, 5-19.

Manselli, P. & Vessella, S., 1991. On Continuous Dependence, on Noncharacteristic Cauchy Data, for Level Lines of Solutions of the Heat Equation, *Forum Math.*, **3**, 513-521.

Mauersberger, P., 1952. Betrachtungen über die zeitliche Änderung der Parameter des geomagnetischen Feldes auf Grund der vorliegenden Potentialentwicklungen. *Abhandlungen Geophysikalisches Institut Potsdam*, No.5, pp. 5-58.

Mauersberger, P., Lucke, O., Lauterbach, R. & Fröhlich, F., 1959. Über das aus dem Erdinnern stammende Magnetfeld. In: Fanselau, G., (ed.), Geomagnetismus und Aeronomie, Band III. Deutscher Verl. d. Wiss., Berlin.

McDonald, K. L., 1957. Penetration of the geomagnetic secular field through a mantle with variable conductivity, *J. Geophys. Res.*, **62**, 117-141.

Munk, W. & Revelle, R., 1952. On the geophysical interpretation of irregularities in the rotation of the Earth, *Mon. Not. R. astr. Soc. Geophys. Suppl.*, No. 6, 331-343.

Plato, R., 1995. Iterative and parametric methods for linear and ill-posed problems, Habilitationsschrift, Fachbereich Mathematik, Technical University Berlin, 85 pages.

Poirier, J.-P. & Le Mouël, J.-L., 1992. Does infiltration of core material into the lower mantle affect the observed geomagnetic field? *Phys. Earth. Planet. Inter.*, **73**, 29-37.

Scientific Technical Report STR 99/12
DOI: 10.2312/GFZ.b103-99127

Reinhardt, H.-J. & Seiffarth, F., 1993. On the Approximate Solution of Illposed Cauchy Problems for Parabolic Differential Equations. In: Anger, G., *et al.*, (eds.), Inverse Problems: Principles and Applications in Geophysics, Technology, and Medicine. Mathematical Research Vol. 74. Akademie-Verlag, Berlin, pp. 284-298.

Rikitake, T., 1973. Global electrical conductivity of the Earth, *Phys. Earth. Planet. Inter.*, **7**, 245-250.

Rochester, M. G., 1960. Geomagnetic westward drift and irregularities in the Earth's rotation, *Phil. Trans. R. Soc. Lond.*, **A252**, 531-555.

Rotanova, N. M., Papitashvili, N. E., Pushkov, A. N. & Fishman, V. M., 1985. Spectral-statistical spatial analysis of 60- and 30-year geomagnetic field variations and conductivity of the lower mantle, *Ann. Geophysicae*, **3**,225-238.

Ryshik, I.M. & Gradstein, I.S., 1963. Summen-, Produkt- und Integraltafeln, Deutscher Verlag d. Wiss., Berlin.

Shankland, T. J., Peyronneau, J. & Poirier, J.-P., 1993. Electrical conductivity of the Earth's lower mantle *Nature*, **366**, 453-455.

Smylie, D. E., 1965. Magnetic Diffusion in a Spherically-Symmetric Conducting Mantle, *Geophys. J. R. astr. Soc.*, **9**, 169-184.

Stix, M., 1982. On electromagnetic core-mantle coupling, *Geoph. Astroph. Fluid Dyn.*, **21**, 303-313.

Stix, M. & Roberts, P. H., 1984. Time-dependent electromagnetic core-mantle coupling. *Phys. Earth Planet. Inter.*, **36**, 49-60.

Stromeyer, D., 1983. Methodische Untersuchungen zur Inversion geothermischer Daten. Diss. Forschungsbereich Geo- und Kosmoswissenschaften, Akad. Wiss. d. DDR, Potsdam, 82 pages.

Stromeyer, D., 1984. Downward Continuation of Heat Flow Data by means of the Least Squares Method. *Tectonophysics* **103**, 55–66.

Tsutsumi, A., 1965. A Remark on the Uniqueness of the Noncharacteristic Cauchy Problem for Equations of Parabolic Type, *Proc. Japan Acad. Ser. A Math. Sci.* **41**, 65–70.

Voorhies, C.V. & Nishihama, M. 1994. Simulaneous solution for core magnetic field and fluid flow beneath an electrically conducting mantle, *J. Geophys. Res.* **99**, B4, 6685-6693.

Whaler, K. A. & Davis, R. G., 1997. Probing the Earth's Core with Geomagnetism, in: Earth's Deep Interior. The Doornbos Memorial Volume. Ed. by D. J. Crossley. Gordon & Breach Science Publ., Amsterdam, pp. 115-166.

Scientific Technical Report STR 99/12
DOI: 10.2312/GFZ.b103-99127

APPENDIX A

An example for the analytical solution of the forward problem

In this appendix and the next one, we are concerned with the analytical solution of the forward problem (standard boundary value problem) and will describe the characteristic difficulties of the inverse problem. We adopt eq.(2) for the conductivity distribution in the conducting shell.

In the forward problem, the time dependence must be prescribed on two boundaries: on the inner boundary, e.g., by a function derived from outer core dynamics (e.g. Braginsky 1984) and on the outer boundary by the time variations calculated for R_σ and given on R_E determined via (15), (16) and (17).

Using the abbreviation $u(r,t) = S^{c,s}_{nm}(r,t)$ we solve the differential equation (12) with a separation ansatz

$$u(r,t) = \tilde{f}(r)\,\tilde{g}(t) = f(x)\,g(t') \tag{39}$$

introducing the normalized variables x, t' defined by

$$r = xR_c \quad \text{and} \quad t = t'\,\mu_0\sigma_0 {R_c}^2, \tag{40}$$

respectively. The separation of eq. (12) leads to $\dot{g}/g = -k^2$, where k is a (complex) constant. The governing equation for the radial modes denoted by f(r) is then given by

$$f'' + \frac{2}{x}f' + (k^2 x^{-\alpha} - \frac{n(n+1)}{x^2})\,f = 0, \quad \text{with} \quad f' = \frac{df}{dx} \tag{41}$$

where k^2 must be prescribed in the forward problem. The solutions are

$$f = x^{-1/2}[C_1\,J_p(z) + C_2\,J_{-p}(z)], \tag{42}$$

where J_p and J_{-p} are the Bessel functions of first kind (Ryshik & Gradstein 1963) with the argument and the index given by

$$z = \frac{2k}{\alpha - 2}\,x^{-\frac{(\alpha-2)}{2}} \quad , \qquad p = \frac{2n+1}{(\alpha - 2)}. \tag{43}$$

(For the case $\alpha = 2$, where z is singular, as well as for some related references see Greiner-Mai 1986.)

Scientific Technical Report STR 99/12
DOI: 10.2312/GFZ.b103-99127

Next, we determine C_2, in dependence on C_1. Application of the boundary conditions (15) to the solutions (16) and (42) results in the validity of

$$[x_\sigma f' + (n+1) f]_{x=x_\sigma} = 0 \tag{44}$$

at $x_\sigma = R_\sigma/R_c$. Using the condition (44) and the recurrence formula for the Bessel functions, we obtain

$$f(x) = C_1 x^{-\frac{1}{2}} [J_p(z) + \frac{J_{p+1}(z_\sigma)}{J_{-p-1}(z_\sigma)} J_{-p}(z)], \tag{45}$$

where $z_\sigma = z(x_\sigma)$ according to eq. (43). In the forward problem, the remainig complex constant is determined from the boundary conditions at the CMB, i.e. by the field model of the core. Here, for simplicity, we assume that the parameters of the solution, k and C_1, are prescribed. For periodic solutions with a prescribed frequency, ν, we get

$$k = \sqrt{i}\ k_0 = \sqrt{i}\ \sqrt{\nu \mu_0 \sigma_0 R_c^2}. \tag{46}$$

The Bessel functions then have the argument

$$z \sim k_0 e^{i\pi/4} x^{-\frac{\alpha-2}{2}}. \tag{47}$$

For $\alpha = 0$, we obtain the half-integer Bessel functions, the real and imaginary parts of which are the Thomson functions (e.g. Ryshik and Gradstein 1963).
The analytical solution of the forward problem can be used to study the penetration of particular oscillations through the mantle. We show the example of the dipole field (n=1) with prescribed periodic time-dependence and $\alpha = 0$.

If we consider some constant factors by replacing C_1 by a new complex constant C_3 (45) reads

$$f(z) = C_3 z^{-\frac{1}{2}} [J_{\frac{3}{2}}(z) + \tan z_s J_{-\frac{3}{2}}(z)],$$

where $z_\sigma = \sqrt{i}\ k_0 x_\sigma$. First, we decompose the Bessel functions and $\tan z$ into real and imaginary parts using $z = \sqrt{i}\ k_0 x = \frac{1+i}{\sqrt{2}} k_0 x$ and the conventional definitions of the hyperbolic functions by the trigonometric functions of an imaginary argument. After some algebraic operations, we obtain

$$z^{-\frac{1}{2}} J_{\frac{3}{2}}(z) = Re(z) + i\,Im(z), \quad z^{-\frac{1}{2}} J_{-\frac{3}{2}}(z) = Re_1(z) + i\,Im_1(z),$$

with Re, Im, Re_1 and Im_1 given by

$$Re\,(x) = \frac{1}{\sqrt{2\pi}\eta x} (-[\cos \eta x \operatorname{ch} \eta x - \sin \eta x \operatorname{sh} \eta x] + \frac{1}{\eta x} \cos \eta x \operatorname{sh} \eta x),$$

Scientific Technical Report STR 99/12
DOI: 10.2312/GFZ.b103-99127

$$\mathrm{Im}\,(x) = \frac{1}{\sqrt{2\pi\eta x}}\,(+\,[\cos\eta x\,\mathrm{ch}\,\eta x + \sin\eta x\,\mathrm{sh}\,\eta x] - \frac{1}{\eta x}\sin\eta x\,\mathrm{ch}\,\eta x),$$
$$\mathrm{Re}_1\,(x) = \frac{1}{\sqrt{2\pi\eta x}}\,(-\,[\sin\eta x\,\mathrm{ch}\,\eta x + \cos\eta x\,\mathrm{sh}\,\eta x] + \frac{1}{\eta x}\sin\eta x\,\mathrm{sh}\,\eta x),$$
$$\mathrm{Im}_1\,(x) = \frac{1}{\sqrt{2\pi\eta x}}\,(+\,[\sin\eta x\,\mathrm{ch}\,\eta x - \cos\eta x\,\mathrm{sh}\,\eta x] + \frac{1}{\eta x}\cos\eta x\,\mathrm{ch}\,\eta x),$$

where $\eta = k_0/\sqrt{2}$. The constant C_3 and $\tan z_\sigma$ are decomposed as follows:

$$C_3 = c\,e^{i\beta}, \qquad \tan z_s = h + i\,q,$$

with

$$h = \frac{\sin\eta x_\sigma \cos\eta x_\sigma}{\cos^2\eta x_\sigma\,\mathrm{ch}^2\,\eta x_\sigma + \sin^2\eta x_\sigma\,\mathrm{sh}^2\,\eta x_\sigma},\ q = \frac{\mathrm{sh}\,\eta x_\sigma\,\mathrm{ch}\,\eta x_\sigma}{\cos^2\eta x_\sigma\,\mathrm{ch}^2\,\eta x_\sigma + \sin^2\eta x_\sigma\,\mathrm{sh}^2\,\eta x_\sigma}.$$

The solution ((12), (39)) u(x,t) = f(x) g(t) can be rewritten as

$$u(x,t) = c\sqrt{w^2(x) + v^2(x)}\,e^{i\,[\varphi(x)+\beta-\nu t]},$$
$$w(x) = \mathrm{Re}(x) + h\,\mathrm{Re}_1(x) - q\,\mathrm{Im}_1(x), \qquad v(x) = \mathrm{Im}(x) + q\,\mathrm{Re}_1(x) + h\,\mathrm{Im}_1(x),$$
$$\varphi(x) = \arctan\frac{v(x)}{w(x)}$$

where c and β are the prescribed constants. Without loss of generality, the phase of the solution is assumed to be zero at $x = 1$ for $t = 0$, so that $\beta = -\varphi(x = 1) = -\varphi(1)$ holds. Introducing $\gamma(x) = \varphi(x) - \varphi(1)$ the associated solution is then given by

$$u(x,t) = c\sqrt{w^2(x) + v^2(x)}\,e^{i\,[\gamma(x)-\nu t]},$$
$$\gamma(x) = -\arctan\frac{v(x)w(1) - w(x)v(1)}{w(x)w(1) + v(x)v(1)},$$

which is suitable to study the penetration of a particular oscillation through the mantle. The solution at any $x > 1$ then becomes phase-shifted by $\gamma(x)$. The normalized amplitude is given by

$$A_\sigma(x) = \sqrt{[w^2(x) + v^2(x)]/[w^2(1) + v^2(1)]}.$$

In the following we give numerical examples of the behaviour of the phase and the normalized amplitude of the poloidal dipole mode as a function of x for the

Scientific Technical Report STR 99/12
DOI: 10.2312/GFZ.b103-99127

10- and 60-year periods. For a shell of 2000 km thickness and $\sigma_M = \sigma_0 = 100\,Sm^{-1}$, the associated parameters of this model are $k_0 \approx 5.5$ and ≈ 2.3, respectively, and $x_\sigma \approx 1.58$. The results are shown in fig. 3a and b. The attenuation (geometrical and inductive) of the modes depends on the frequency considered, and the shape of the amplitude spectra of a particular spherical harmonic mode depends on x. For example, a spectrum which shows equal amplitudes for different periods at the CMB is transformed into a spectrum at $r = R_E$ where the amplitudes increase with increasing period, which is typical for a low-pass filter. The forward solution therefore shows that the mantle induction must be taken into account if the observed amplitude distribution is to be interpreted by, e.g., core-mantle coupling. As shown in figure 3b, the conductivity also causes a phase lag between $x = 1$ and $x = x_\sigma$, which is lower for the higher period, and becomes negligible if the period continues to increase. In particular, this will be important for the interpretation of the phase lag between geomagnetic field quantities and ΔLOD. Phase differences can also appear for magnetic variations, which have equal periods and are associated with modes of different number n.

Scientific Technical Report STR 99/12
DOI: 10.2312/GFZ.b103-99127

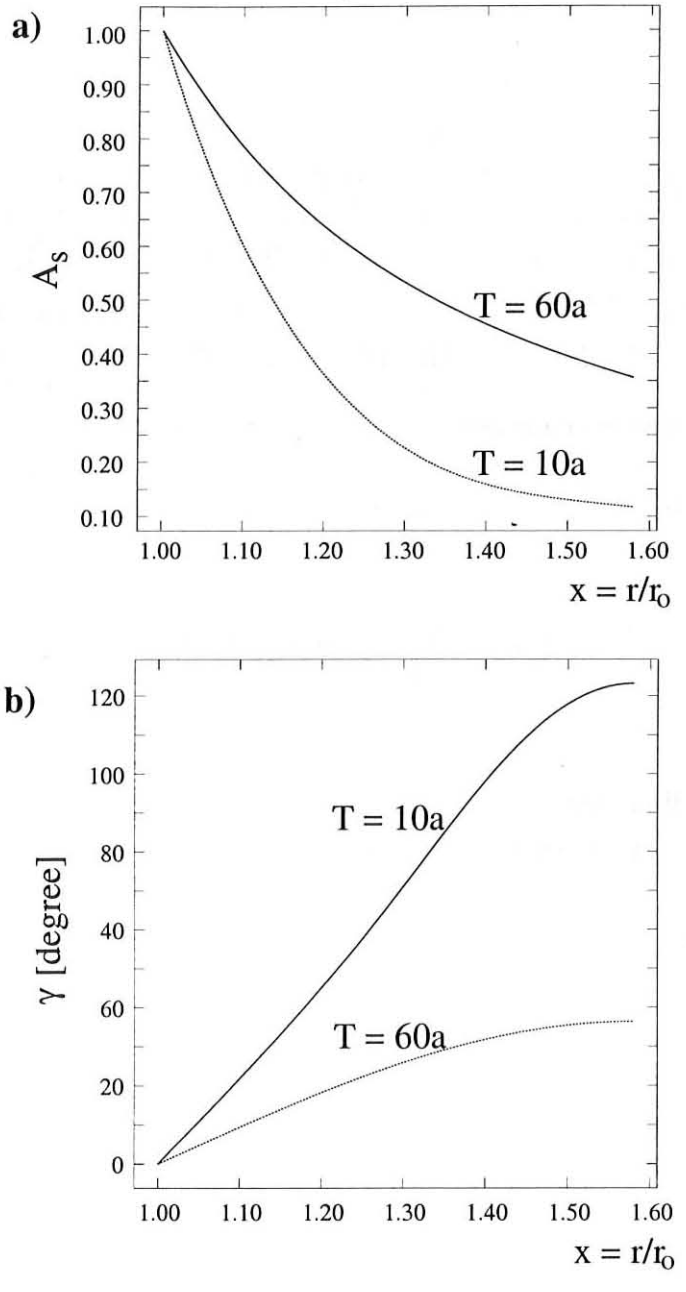

Figure 3: (a) Relative amplitude A_s and (b) phase γ of the poloidal dipole modes as a function of $x = r/r_0$ for the 10- and 60-year periods and $\sigma_M = 100\,Sm^{-1}$ in a shell of 2000 km thickness (r_0 core radius).

Scientific Technical Report STR 99/12
DOI: 10.2312/GFZ.b103-99127

APPENDIX B

Remarks on the inverse problem

For the analytical forward problem (two-side standard boundary value problem) presented in Appendix A also an associated (analytical) inverse boundary problem can be studied. With (15), (16) and (17) the time variation of the considered magnetic field component at R_σ, abbreviated here, as above, by $\phi(t)$, is related to the boundary values by

$$\phi(t) = S^{c,s}_{nm}(R_\sigma, t) = C^{c,s}_{nm}(t)\, {R_\sigma}^{-n-1} \tag{48}$$

and can be obtained from the observations. Eq.(45) continues to be valid, but now $C_1(k)$ is an unknown function and has to be determined from the continuity of the solutions (16) and (45) at $x = x_\sigma$. We obtain as solution in our example with $\alpha = 0$ and $n = 1$ an integral representation for $u(x,t) = f(r)g(t')$:

$$u(x,t') = \lim_{(a,b)\to\infty} \int_{-(a+ib)}^{a+ib} C_1(k)\, e^{-k^2 t'} (kx)^{-\frac{1}{2}} \left[J_{\frac{3}{2}}(kx) + \tan kx_\sigma\, J_{-\frac{3}{2}}(kx)\right] dk \tag{49}$$

which describes the inverse problem for $C_1(k)$ as solution of a Fredholm integral equation of the first kind.

The boundary condition for $x = x_\sigma$ then gives

$$\phi(t') = -\sqrt{\frac{\pi}{2}} \lim_{(a,b)\to\infty} \int_{-(a+ib)}^{a+ib} \frac{C_1(k)}{kx_\sigma \cos kx_\sigma}\, e^{-k^2 t'}\, dk \ . \tag{50}$$

If we take into account higher modes (n=1,2,3...) and $\alpha \neq 0$, the kernel of this integral will be still more complicated (see eq. (45)).

Let us write $k^2 = \mu_1 + i\nu_1$. A first physical condition is then associated with the observed slow decrease of the dipole field over a long period. Because the mantle is a conducting shell without internal dynamics, we conclude that $\mu_1 \geq 0$ is valid within the mantle. In addition, the values of μ_1 must be finite. For a weakly conducting mantle, the time-dependent potential field is usually assumed to be a first order approximation of the exact solution. Considering the normalized time scale and the decrease of the axial dipole field of about $20\mathrm{nTa}^{-1}$, we find that μ_1 is in the order of 10^{-3} if the potential solution is applicable. So we have a first approximation for μ_1. The frequency ν_1 is constrained by the assumption

Scientific Technical Report STR 99/12
DOI: 10.2312/GFZ.b103-99127

of decade oscillations, so that ν_1 is in the interval [0.3, 3.0] for the conductivity model used. Therefore, we can assume that the area of integration is a small rectangle in the complex k plane. An additional constraint can be obtained if the conductivity is constant or decreases monotonously from the CMB towards R_σ, e.g. according to the setups (1) and (2). Because the magnetic field has no sources in the mantle, the flux density also decreases monotonously. The smallest decrease is shown by the potential field, which reflects the geometrical weakening of the field if the conductivity is zero. In reality, inductive weakening according to the loss of energy by ohmic dissipation is superimposed. In the inverse boundary value problem, the potential solution gives the lowest amplification of the field continued towards the CMB. If $\sigma_M \neq 0$, then the upper bound of amplification of the modes cannot be specified. For example, modes of high frequencies are not observed because of their strong attenuation. However, they may exist at the CMB, so that the inverse solution cannot be applied to this frequency domain (the amplification will then be infinite). Finally, the modes of higher order can only be estimated with large statistical errors at the earth surface. These errors are strongly amplified when continued to the CMB.

It can be estimated that arbitrarily small errors in the data function can result in arbitrarily large disturbances in the unknown function on the core-mantle boundary. To show this, we consider here only the case $\alpha = 0$ and $n = 1$ for the conductivity law (2) and the differential equation (19) (section 3.1), respectively, i.e. the behaviour of the dipole field in a mantle with constant conductivity.

We take $|\phi(t) - \phi^\delta(t)| \leq \delta$ with $\phi(t)$ as "exact" data and $\phi^\delta(t) = \phi(t) + \delta \sin\nu t$ as "disturbed" data. Inserting this in the differential equation (19), we find the estimate (using also Appendix A)

$$|u(r,t) - u^\delta(r,t)| \geq C\frac{\delta}{\nu^{1/2}\, r}\exp((\nu/2)^{1/2}r), \quad R_c \leq r \leq R_\sigma. \tag{51}$$

Thus, we see how a data error δ is amplified in dependency of its frequency content ν. Because high-frequency disturbances in the data cannot be excluded, large errors in the results are possible only limited by the Nyquist frequency. Therefore, additional mathematical and physical constraints of the inverse solution should be introduced in the future, e.g. constraints inferred from the magnitude of the electromagnetic torques necessary to excite the ΔLOD.

Scientific Technical Report STR 99/12
DOI: 10.2312/GFZ.b103-99127

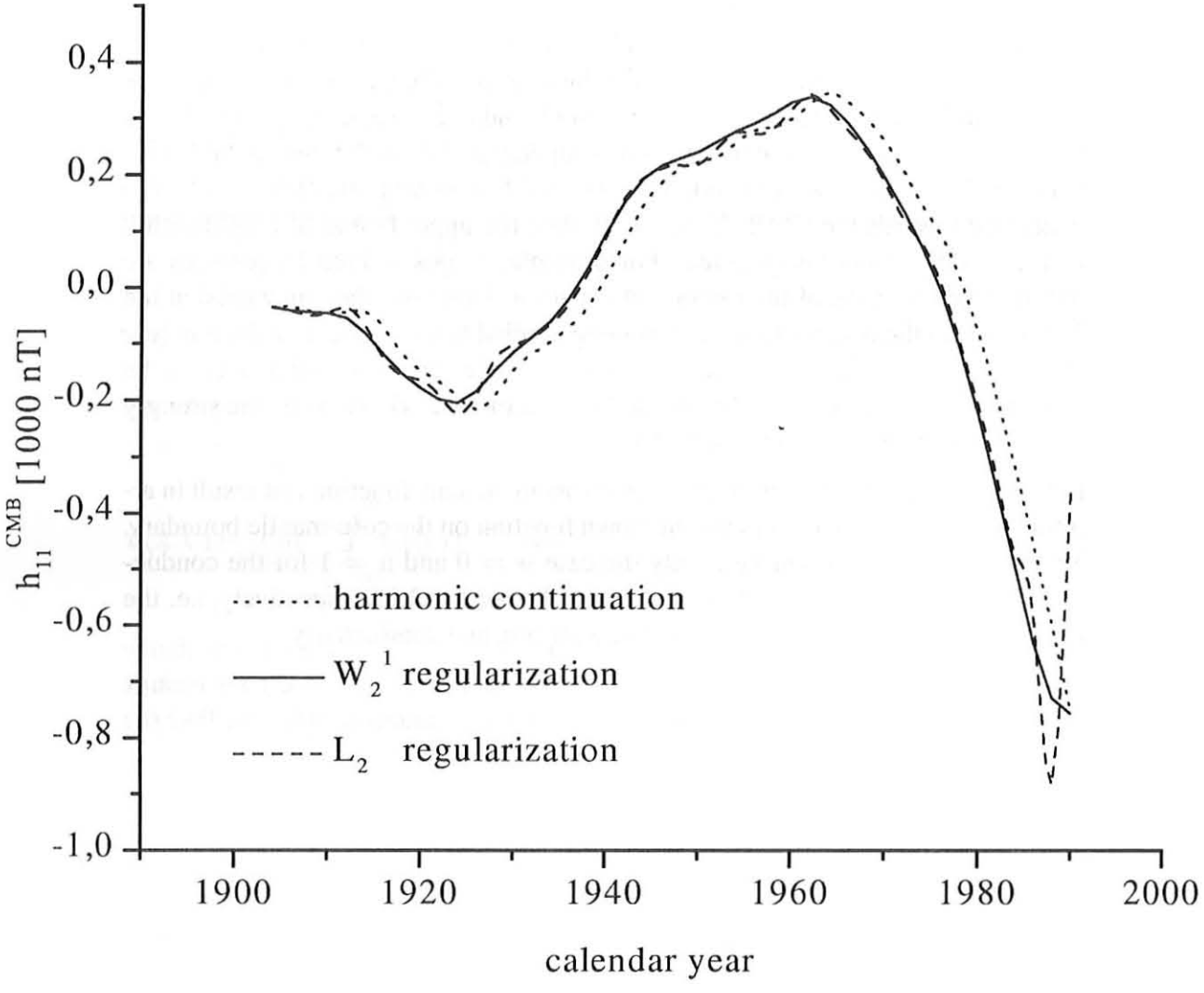

Figure 4: Downward continuation of the Gauss coefficient $h_{11}(t)$ onto the CMB: Solutions h_{11}^{CMB} by regularization with the $\|u(R_c, .)\|_2$ norm and the $\|u(R_c, .)\|_{W_2^1}$ norm, using the conductivity model σ_{M_1} from table 1, and by harmonic downward continuation. Linear trends are removed.

Scientific Technical Report STR 99/12
DOI: 10.2312/GFZ.b103-99127

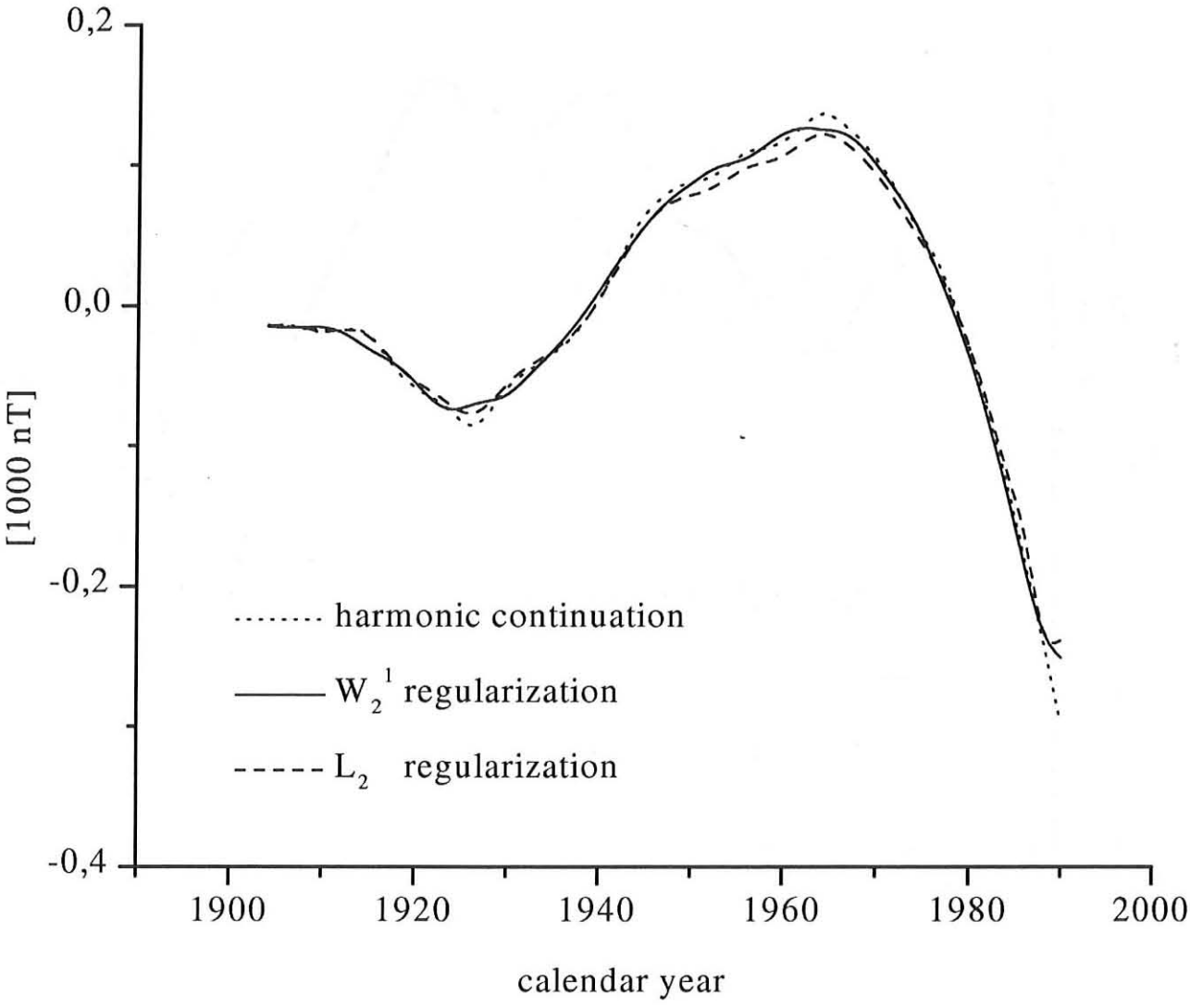

Figure 5: Downward continuation of the Gauss coefficient $h_{11}(t)$ onto the CMB: Comparison at R_σ of the data ("harmonic continuation") with the regularized solutions which were calculated for the conductivity model σ_{M_1} from table 1 and with the $\|u(R_c, .)\|_2$ norm and the $\|u(R_c, .)\|_{W_2^1}$ norm, respectively. Linear trends are removed.

Scientific Technical Report STR 99/12
DOI: 10.2312/GFZ.b103-99127

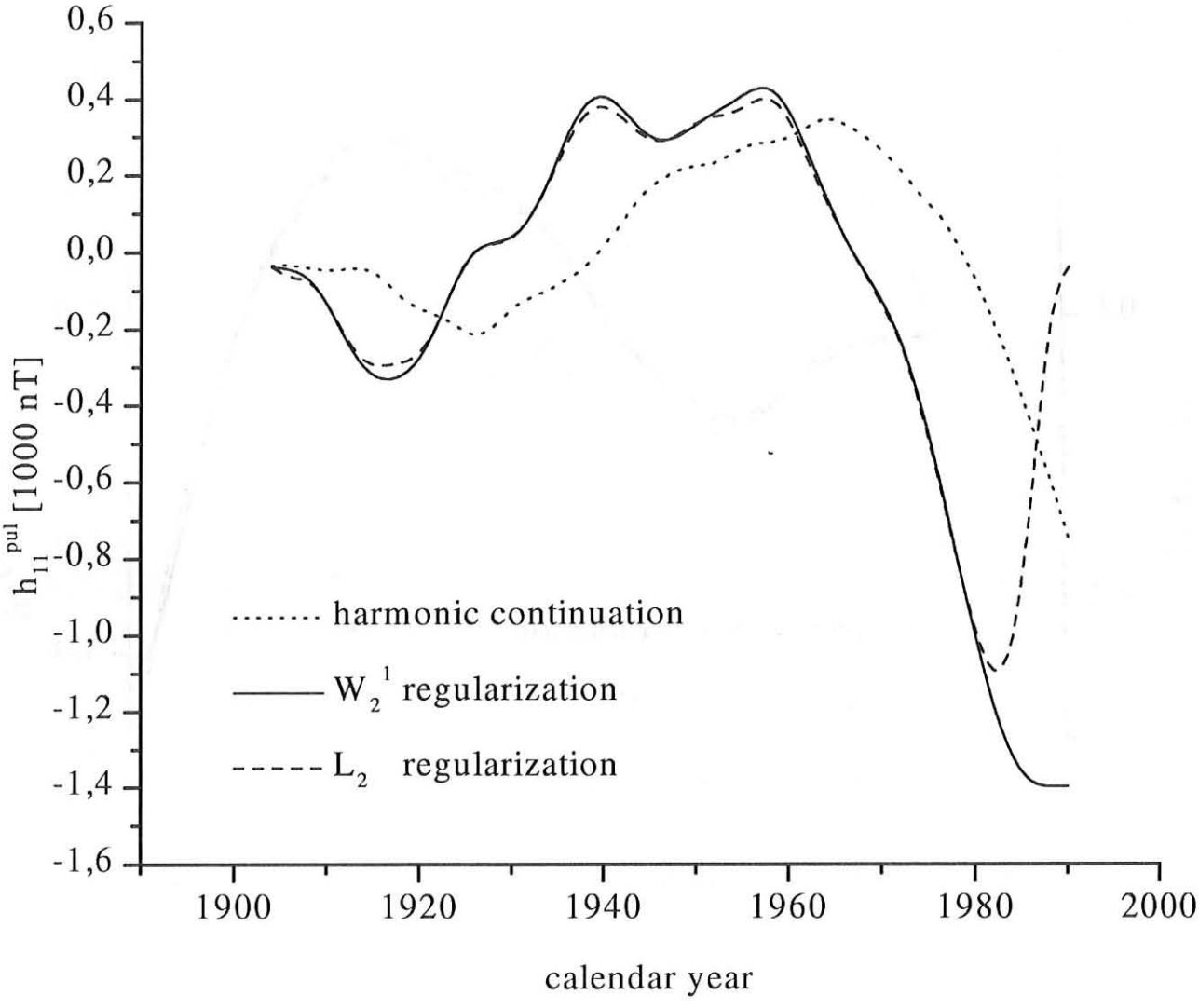

Figure 6: Downward continuation of the Gauss coefficient $h_{11}(t)$ into the passive upper core layer ($R_c - 50km$) : Solutions h_{11}^{pul} by regularization with the $\|u(R_c, .)\|_2$ norm and the $\|u(R_c, .)\|_{W_2^1}$ norm, using the conductivity models σ_{M_1} and σ_{pul} from table 1, and by harmonic downward continuation. Linear trends are removed.

Scientific Technical Report STR 99/12
DOI: 10.2312/GFZ.b103-99127

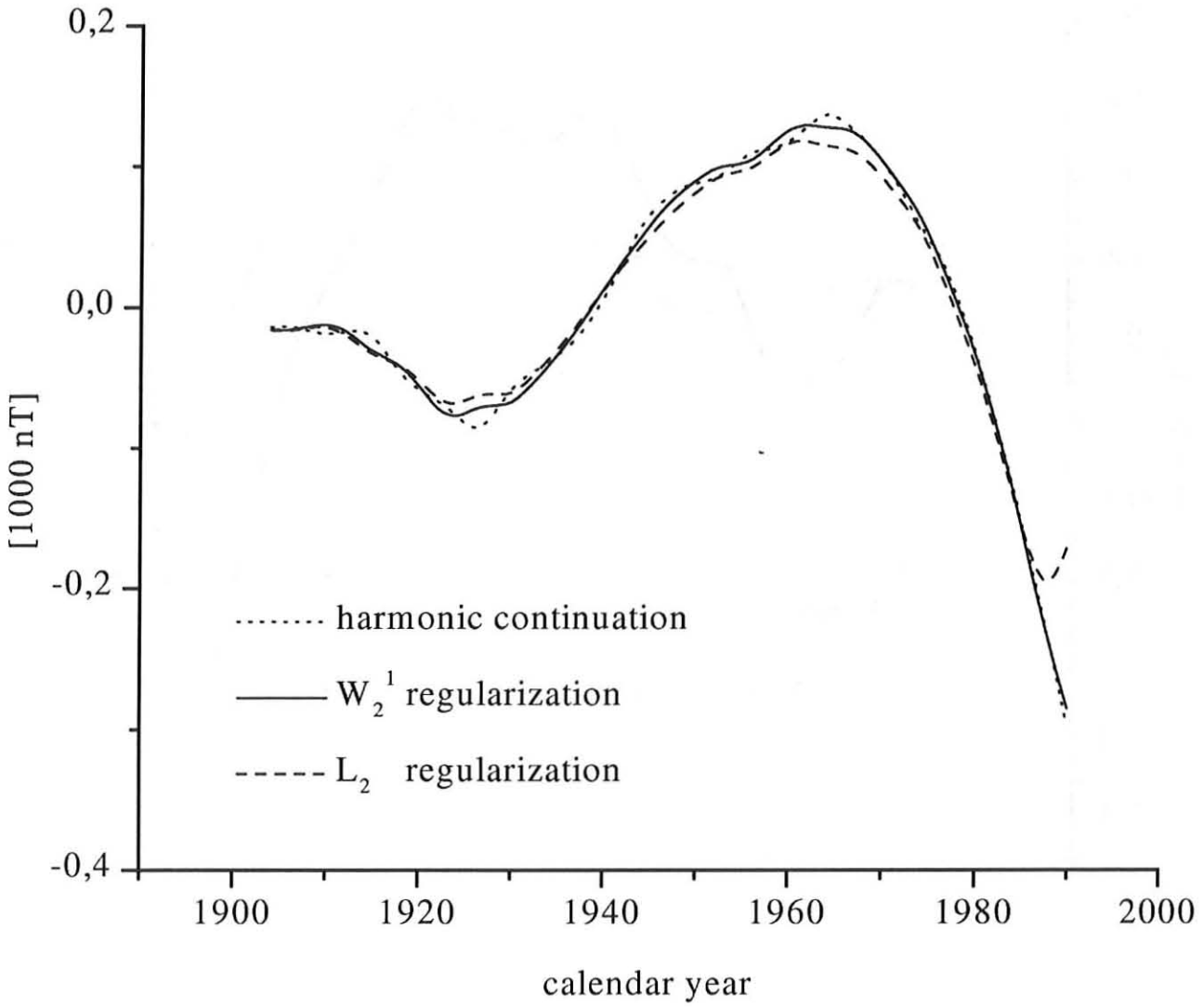

Figure 7: Downward continuation of the Gauss coefficient $h_{11}(t)$ into the passive upper core layer ($R_c - 50km$) : Comparison at R_σ of the data ("harmonic continuation") with the regularized solutions which were calculated for the conductivity models σ_{M_1} and σ_{pul} from table 1 and with the $\|u(R_c, .)\|_2$ norm and the $\|u(R_c, .)\|_{W_2^1}$ norm, respectively. Linear trends are removed.

Scientific Technical Report STR 99/12
DOI: 10.2312/GFZ.b103-99127

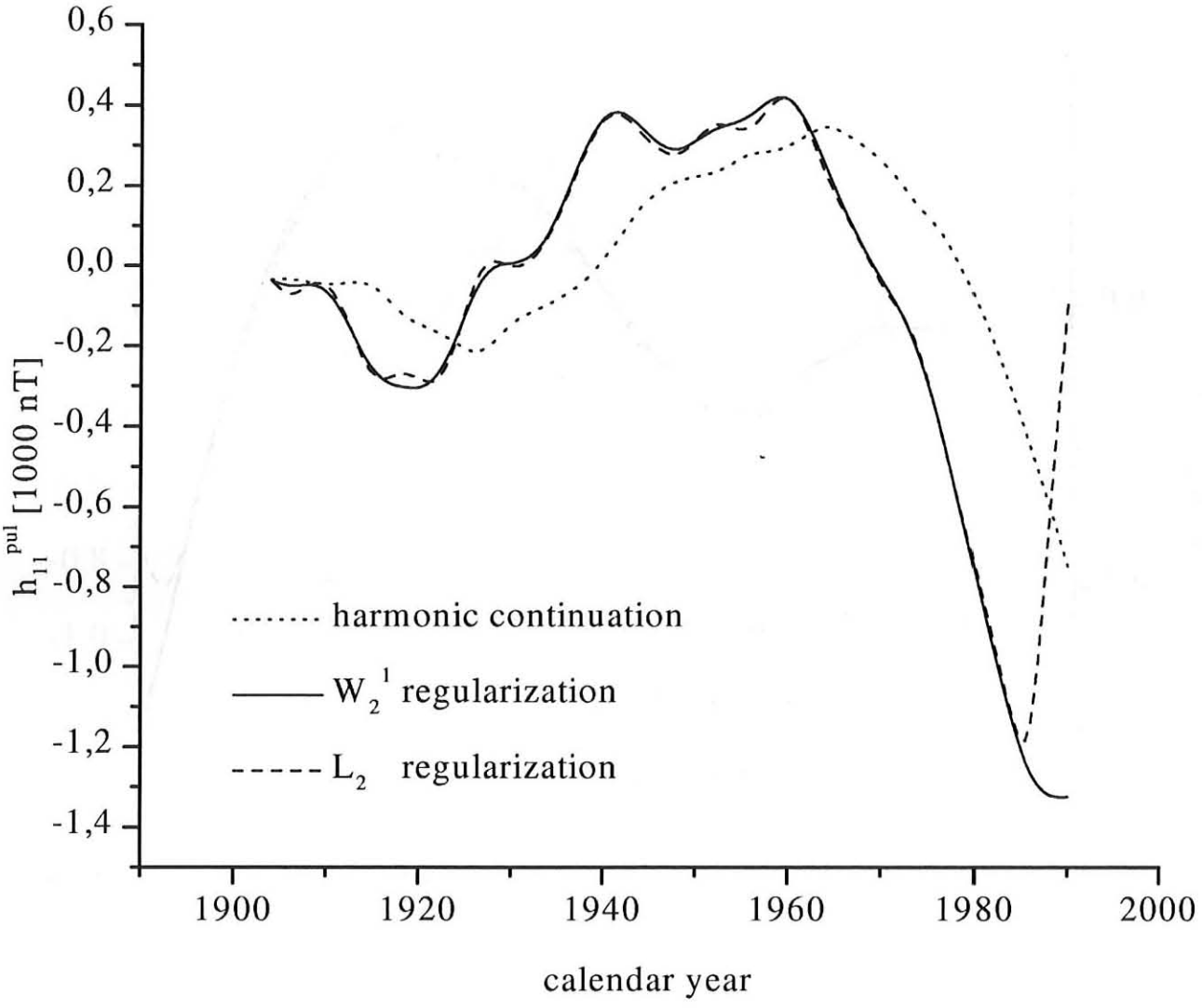

Figure 8: Downward continuation of the Gauss coefficient $h_{11}(t)$ into the passive upper core layer ($R_c - 50km$) : Solutions h_{11}^{pul} by regularization with the $\|u(R_c, .)\|_2$ norm and the $\|u(R_c, .)\|_{W_2^1}$ norm, using the conductivity models σ_{M_2} and σ_{pul} from table 1, and by harmonic downward continuation. Linear trends are removed.

Scientific Technical Report STR 99/12
DOI: 10.2312/GFZ.b103-99127

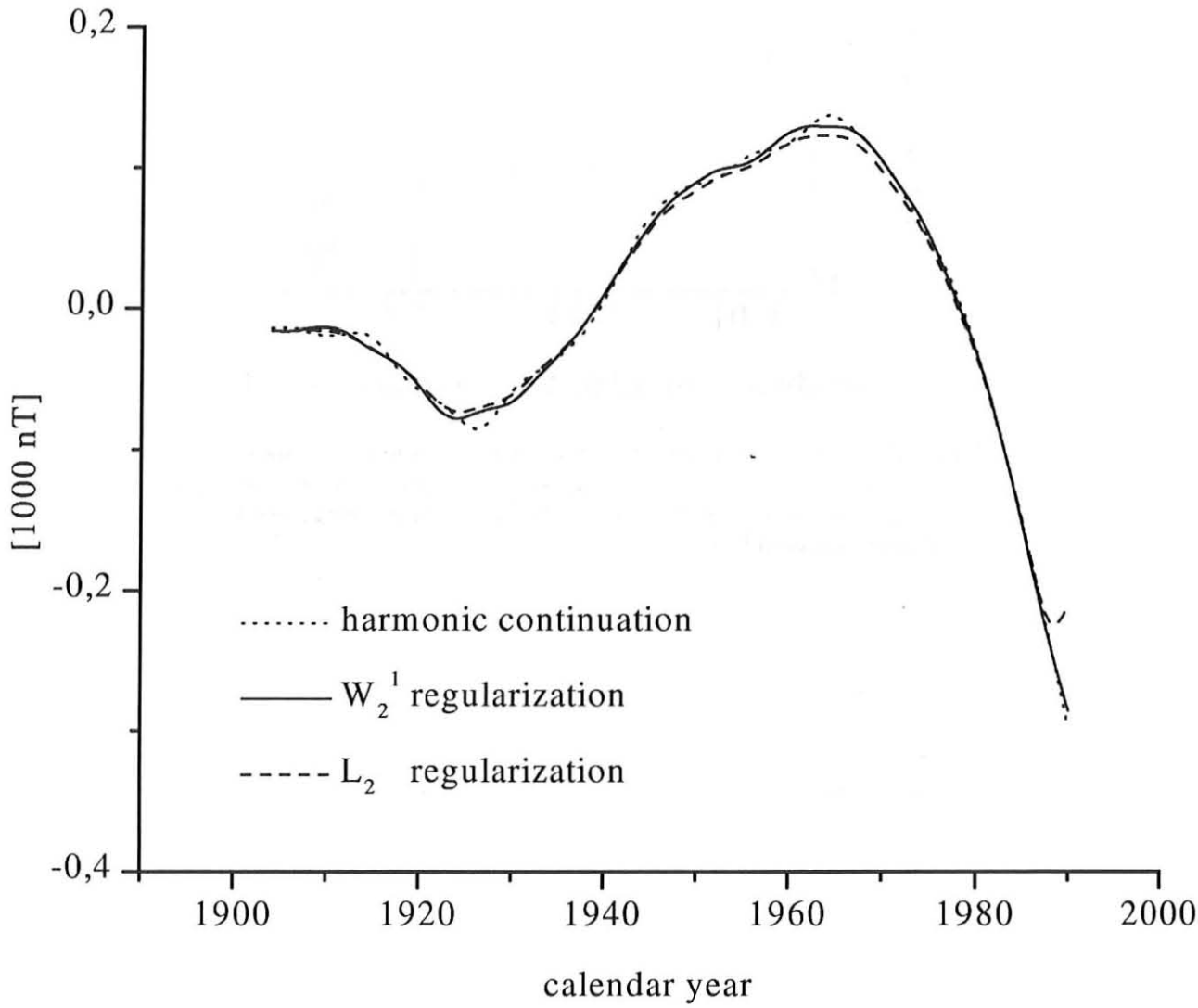

Figure 9: Downward continuation of the Gauss coefficient $h_{11}(t)$ into the passive upper core layer ($R_c - 50km$) : Comparison at R_σ of the data ("harmonic continuation") with the regularized solutions which were calculated for the conductivity models σ_{M_2} and σ_{pul} from table 1 and with the $\|u(R_c, .)\|_2$ norm and the $\|u(R_c, .)\|_{W_2^1}$ norm, respectively. Linear trends are removed.

Scientific Technical Report STR 99/12
DOI: 10.2312/GFZ.b103-99127

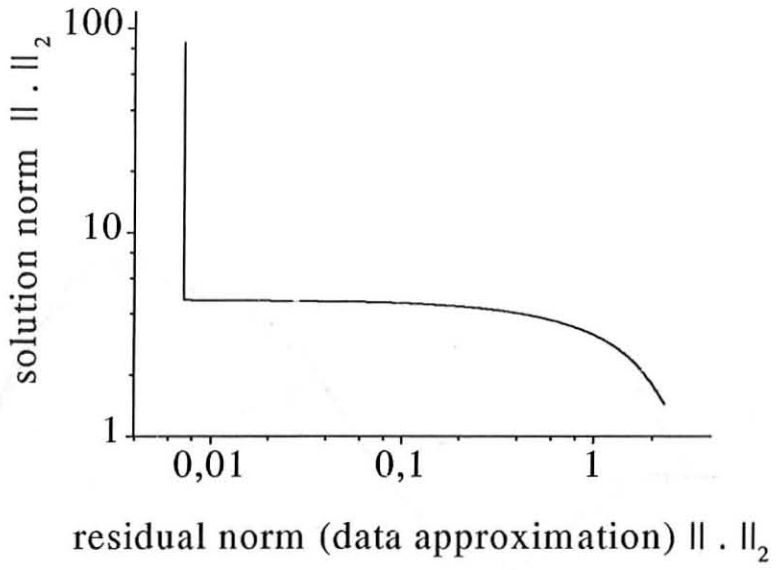

Figure 10: L-curve for Tikhonov regularization applied to the downward continuation of the Gauss coefficient h_{11} onto the CMB, using the solution norm $\|u(R_c,.)\|_2$, the conductivity model σ_{M_1} from table 1 and the residual norm $\|.\|_2$ (data approximation at R_σ)

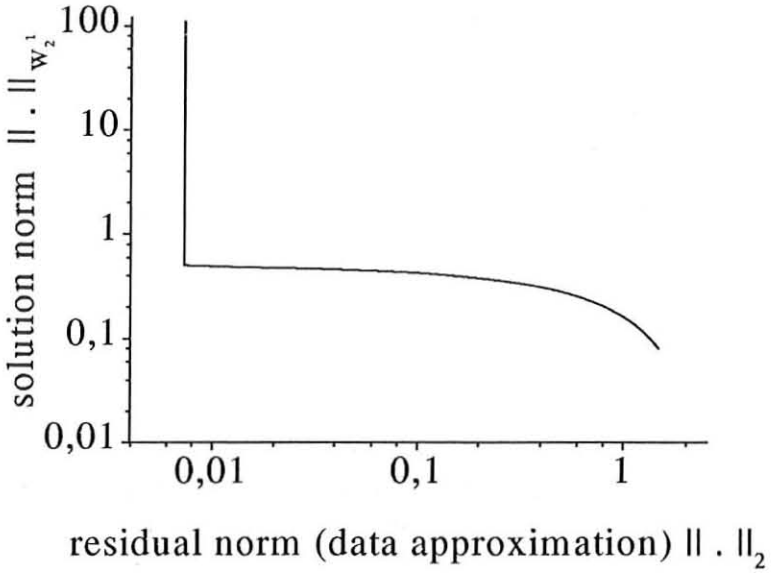

Figure 11: L-curve for Tikhonov regularization applied to the downward continuation of the Gauss coefficient h_{11} onto the CMB, using the solution norm $\|u(R_c,.)\|_{W_2^1}$, the conductivity model σ_{M_1} from table 1 and the residual norm $\|.\|_2$ (data approximation at R_σ)

Scientific Technical Report STR 99/12
DOI: 10.2312/GFZ.b103-99127

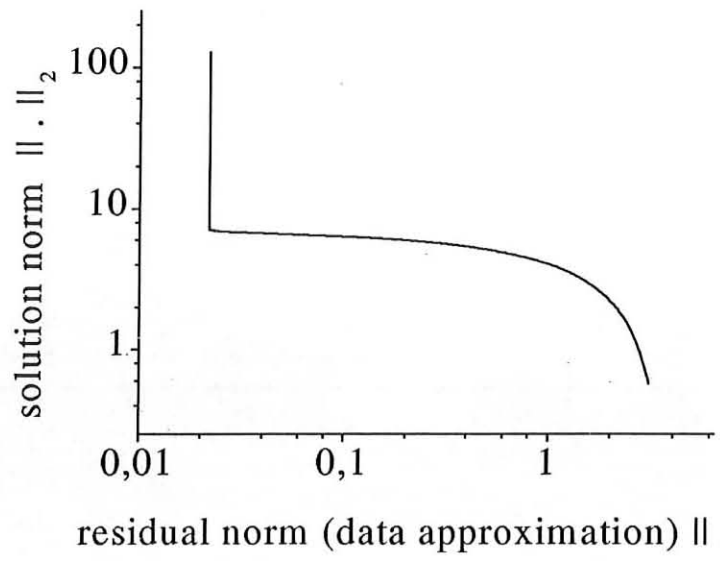

Figure 12: L-curve for Tikhonov regularization applied to the downward continuation of the Gauss coefficient h_{11} into the passive upper core layer ($R_c - 50$km), using the solution norm $\|u(R_c, .)\|_2$, the conductivity models σ_{M_1} and σ_{pul} from table 1 and the residual norm $\|.\|_2$ (data approximation at R_σ)

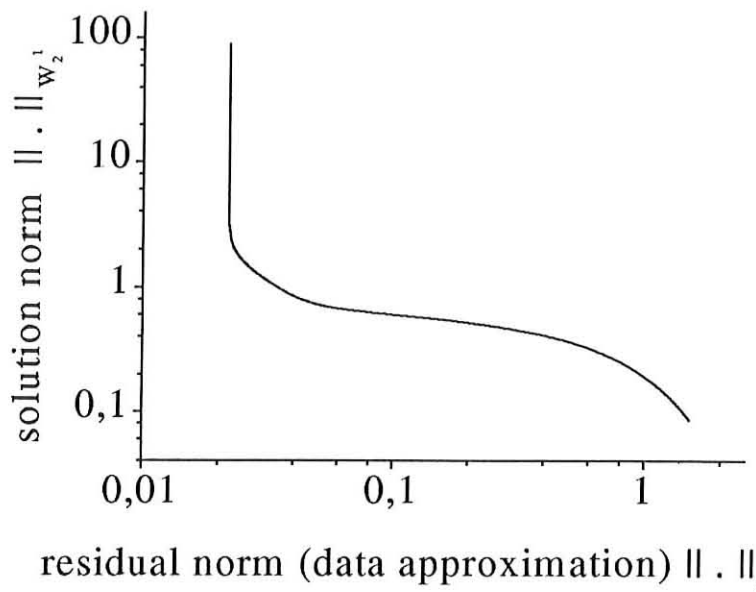

Figure 13: L-curve for Tikhonov regularization applied to the downward continuation of the Gauss coefficient h_{11} into the passive upper core layer ($R_c - 50$km), using the solution norm $\|u(R_c, .)\|_{W_2^1}$, the conductivity models σ_{M_1} and σ_{pul} from table 1, and the residual norm $\|.\|_2$ (data approximation at R_σ)

Scientific Technical Report STR 99/12
DOI: 10.2312/GFZ.b103-99127

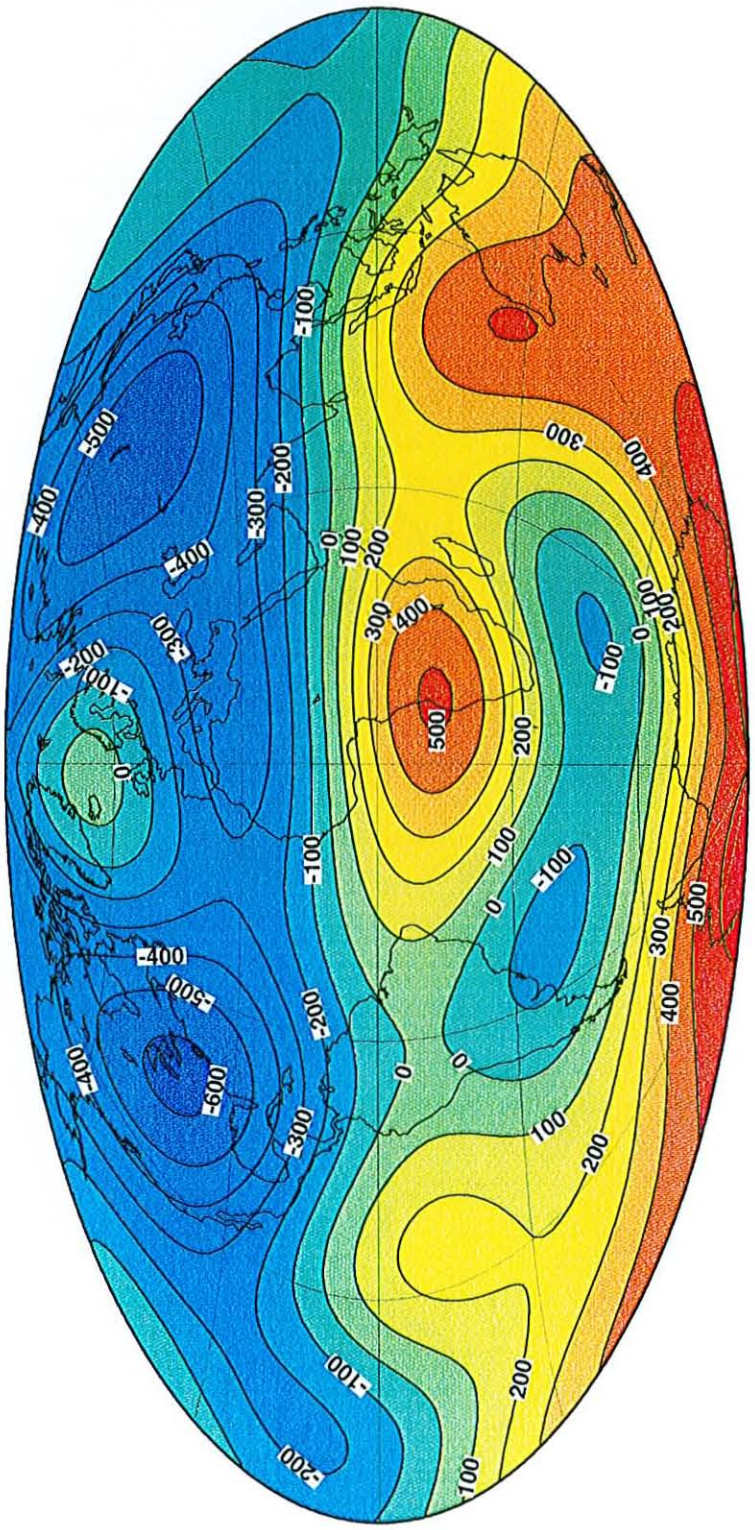

Figure 14: Radial component B_r of the (5,5) magnetic field on the CMB for 1930 calculated with the conductivity model σ_{M_1} and the boundary values g_{nm} and h_{nm} due to Hodder (1981) by means of downward continuation regularized with the $\|u(R_c, .)\|_{W_2^1}$ norm. Values are in units of 1000 nT.

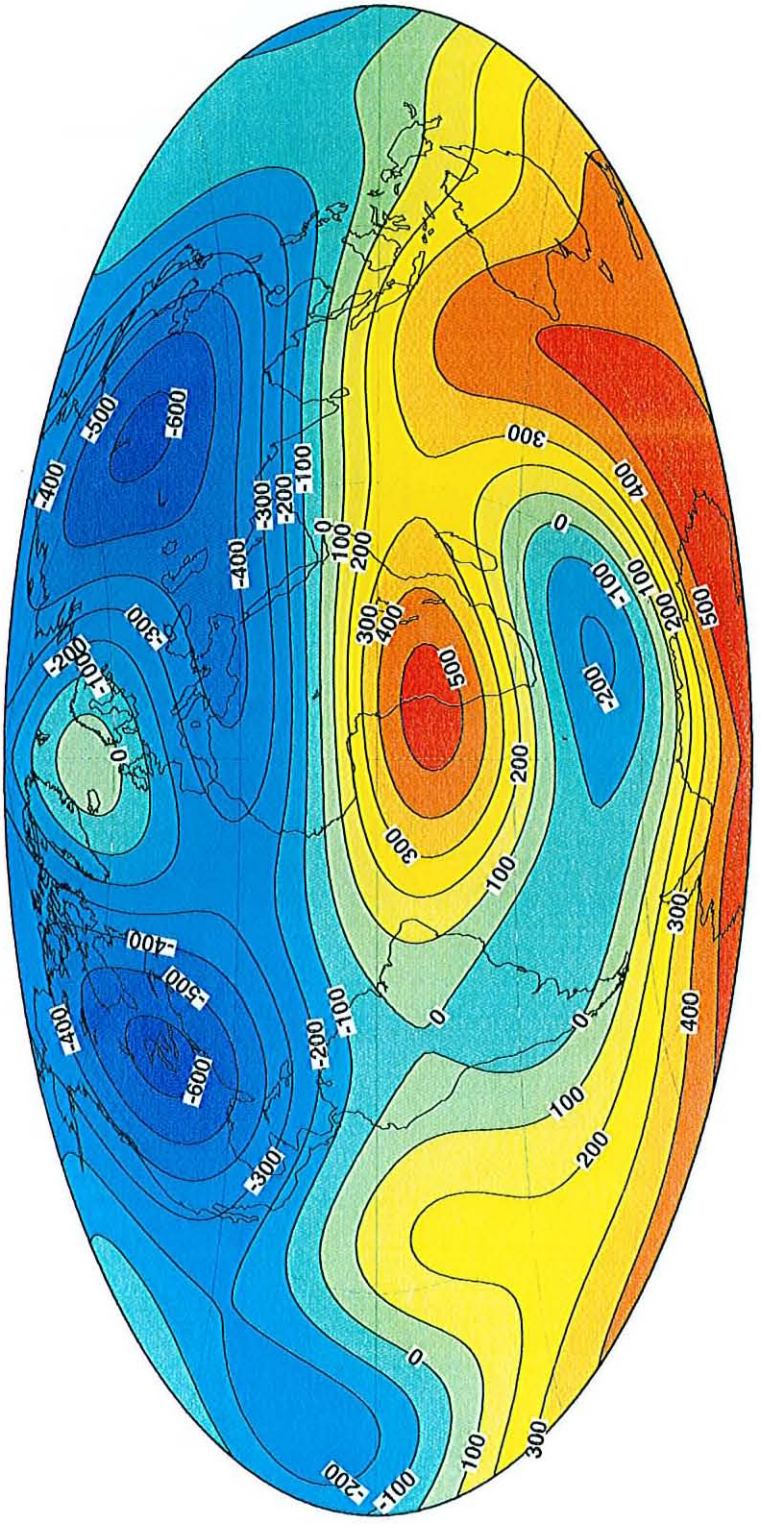

Figure 15: Radial component B_r of the (5,5) magnetic field on the CMB for 1960 calculated with the conductivity model σ_{M_1} and the boundary values g_{nm} and h_{nm} due to Hodder (1981) by means of downward continuation regularized with the $\|u(R_c, .)\|_{W_2^1}$ norm. Values are in units of 1000 nT.

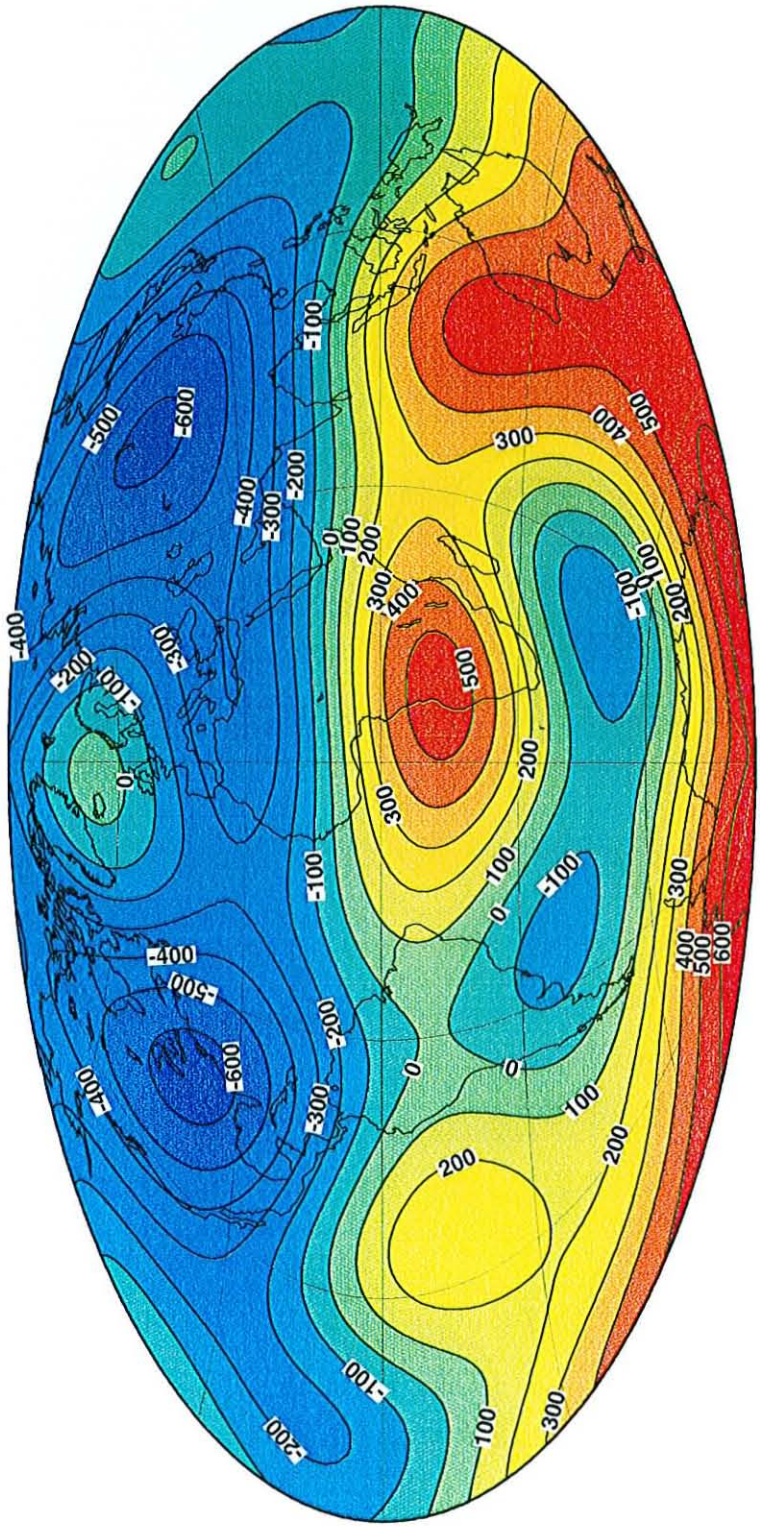

Figure 16: Radial component B_r of the (5,5) magnetic field in the passive upper core layer ($R_c - 50$km) for 1930 calculated with the conductivity models σ_{M_1}, σ_{pul} and the boundary values g_{nm} and h_{nm} due to Hodder (1981) by means of downward continuation regularized with the $\|u(R_c, .)\|_{W_2^1}$ norm. Values are in units of 1000 nT.

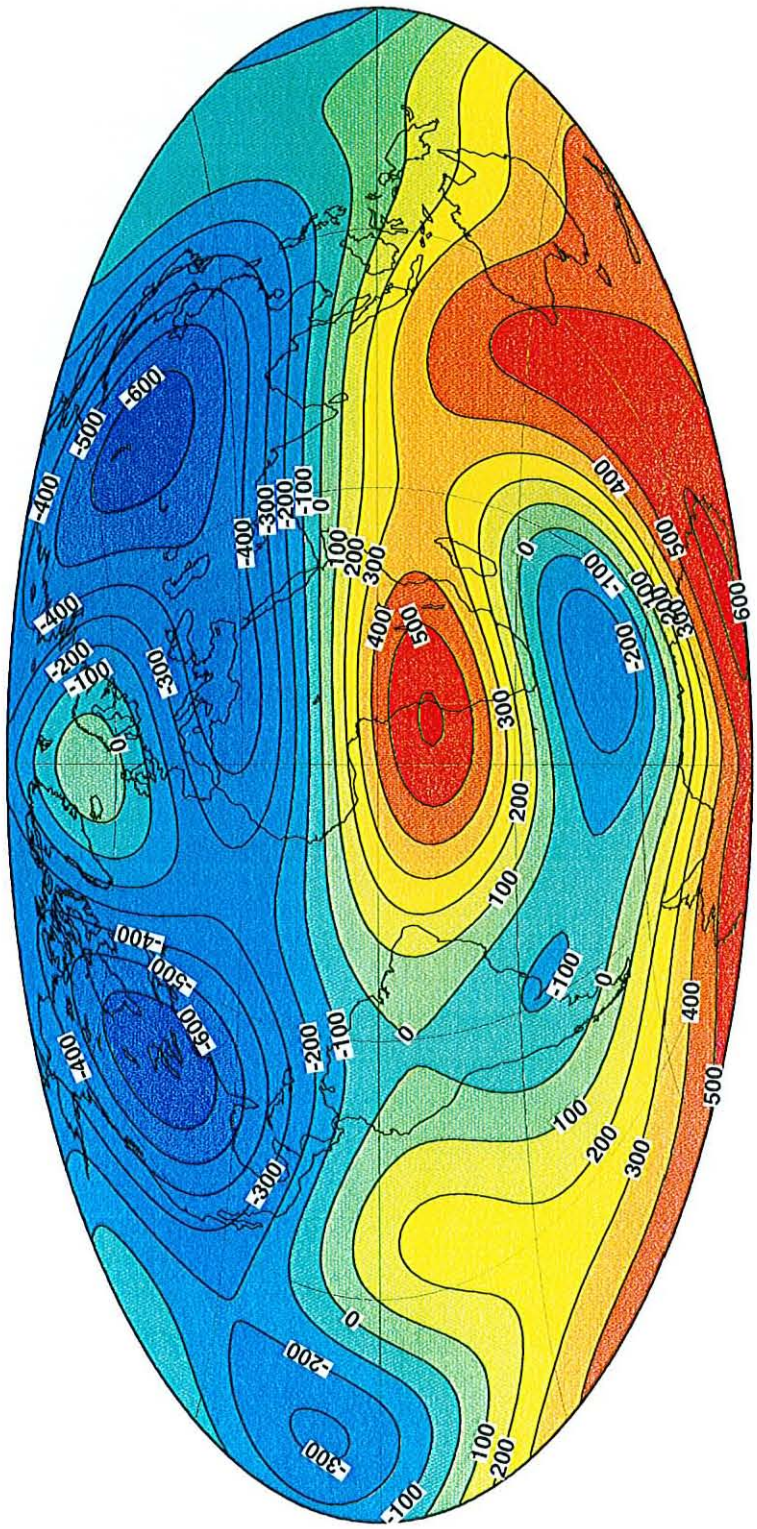

Figure 17: Radial component B_r of the (5,5) magnetic field in the passive upper core layer ($R_c - 50$km) for 1960 calculated with the conductivity models σ_{M_1}, σ_{pul} and the boundary values g_{nm} and h_{nm} due to Hodder (1981) by means of downward continuation regularized with the $\|u(R_c, .)\|_{W_2^1}$ norm. Values are in units of 1000 nT.